Tissue electroporation as a bioelectric phenomenon: basic concepts.

Abstract. Electroporation is the phenomenon in which cell membrane permeability to ions and macromolecules is increased by exposing the cell to short (microsecond to millisecond) high electric field pulses. In living tissues, such permeabilization boost can be used in order to enhance the penetration of drugs (electrochemotherapy) or DNA plasmids (electrogenetherapy) or to destroy undesirable cells (irreversible electroporation). The main purpose of the present chapter is to provide an overview of the electrical concepts related to electroporation for those not familiar with electromagnetism. It is explained that electroporation is a dynamic phenomenon that depends on the local transmembrane voltage and it is shown how a voltage difference applied though a pair of electrodes generates an electric field which in turn induces the required transmembrane voltage for electroporation to occur. Quite exhaustive details are given on how electroporation changes the passive electrical properties of living tissues. Furthermore, some remarks are given about the effects of electroporation on other bioelectric phenomena such as cardiac arrhythmias.

1. Introduction

Bioelectricity typically refers to the electromagnetic energy produced by living organisms. Such energy is usually manifested as ionic currents at nerves or muscles due to the propagation of the so called *action potentials*. However, in a broader sense, bioelectricity also refers to the study of the interaction of externally applied electromagnetic energy with living organisms, as it is the case of the electroporation phenomenon.

Like in other bioelectricity topics, electroporation can be approached from a life sciences perspective or from a physical sciences perspective. This duality enriches the topic but also creates some confusion and hinders a comprehensive view of the phenomenon. The present chapter is intended to help to bridge both approaches: its main purpose is to provide an overview of the electrical concepts related to electroporation for those not familiar with electromagnetism. Some advanced aspects are presented that may be of interest for engineers or physicists working in the field (particularly in sections 5 and 6) but electrical terminology and concepts are simplified as much as possible.

Going back to the duality of bioelectricity it is interesting to note that discoveries in electricity and biology have been interlinked throughout the history. For instance, in a series of experiments started in 1780, Luigi Galvani, a physician, discovered that when a dead frog was placed on an iron grating and a bronze hook touched the spinal cord then the frog's muscle twitched. His explanation to the phenomenon was based on what he called *animal electricity*. Later, it was Alessandro Volta, a physicist, who found the correct explanation: the presence of two different metals in the same electrolyte (frog's body fluids) had created a DC current that had stimulated the frog's muscles. That lead to the invention of the voltaic pile (Volta replaced the frog's fluids by brine-soaked paper), which was the first device able to produce steady electric current and that became a basic element for later discoveries in electromagnetism.

In 1925, Fricke [1] produced a result in the opposite direction: two decades before the lipid bi-layer was understood, he was able to hypothesize a reasonable value for the membrane thickness (30 nm instead of the actual 7 nm) by analyzing the passive electrical properties of red blood cells. His calculations were based on an electrical model for the cell, and its environment, in which the cell membrane was modeled as a dielectric layer. Interestingly, from such a model an additional hypothesis could be drawn: some sort of dielectric rupture phenomenon could exist in the case of living tissues as it is manifested in most dielectrics: when a dielectric is subjected to a sufficiently high electric field, some bound electrons are freed and accelerated, then those electrons can liberate additional electrons during collisions in a process called avalanche breakdown. This process leads to a dramatic conductivity increase and, in some cases, to permanent physical damage of the dielectric material. Now it is accepted that electroporation is not due to dielectric rupture by electron avalanche [2] but the idea that membrane breakdown could be caused by excessive transmembrane voltage surely helped to understand some experimental observations that are related to electroporation. At that time, neurophysiology researchers knew that when a certain electrical stimulus threshold was surpassed the electrophysiological manifestations were disrupted. And, for instance, A. L. Hodgkin, who won the 1963 Nobel Prize in Physiology or Medicine for his work with A. F. Huxley on the basis of nerve action potentials, noted in 1951 that the *Ritter's opening tetanus* might be due to the fact that "the insulating properties of the membrane break down under the influence of the abnormally high potential difference" [3]. In 1957, Stämplfi [4] correctly demonstrated the phenomenon as being a disturbance of the cell membrane dielectric properties and noticed that this effect could be reversible under certain circumstances. Since then, multiple scientific discoveries and practical applications of electroporation have emerged. In 1967, Sale and Hamilton [5-7] observed that leakage of intracellular ions and molecules occurs immediately the application of the electric field pulses and, ten years later, Kinosita and Tsong [8] demonstrated that reversible electroporation could also be employed to allow cellular uptake. Then Neumann et al. in 1982 [9] were the first ones to facilitate gene transfer into cells by means of electroporation. This created a powerful method for gene transfection that has been used in microbiology labs for more than 25 years. In the early 90s, Mir pioneered the use of *in vivo* electroporation for the introduction of chemotherapy drugs in solid tumors [10, 11]. And now we are witnessing how *in vivo* irreversible electroporation (IRE) is becoming a new surgical tool able to perform tissue ablation without the drawbacks of thermal methods.

This chapter is organized into seven sections. The first three sections, including the present introduction section, are intended to provide a general overview of some basic concepts that are required to understand electroporation from an electrical point of view. In section 4 it is explained that electroporation occurs when the transmembrane voltage reaches a certain threshold and it is shown how an external electric field induces such transmembrane voltage in cell suspensions and tissues. Furthermore, some basics concepts are given about the use of the

finite element method for simulating the electric field distribution in tissues. The fifth section deals with the dynamic changes that occur in membrane conductance during the application of the electroporation pulse. It is shown how these changes influence the electric current waveform and how relevant these changes can be for computing the electric field distribution. Then, the sixth section describes the changes in conductance that occur after pulse termination. And, finally, the last section very briefly introduces a topic that would require another full chapter and that will probably deserve further future research: the effect of electroporation on other bioelectric phenomena.

2. Overview of basic electricity concepts

This subsection is intended to provide a brief overview of the main concepts on electromagnetism that are required to understand electroporation from an electrical perspective. Those familiar with basic electromagnetism or circuit theory can skip this subsection without hesitation. Readers who feel they require another source to learn the concepts presented here are encouraged to look for the electromagnetism section in any general physics textbook at undergrad level.

Electric charge (Q) is the fundamental property of some subatomic particles that determines their electromagnetic interaction. Positive and negative charges have been defined. The unit used to express the amount of charge is the coulomb (C) and the value of the elementary charge is $+1.602 \times 10^{-19}$ C which is the charge of a proton (charge of an electron = -1.602×10^{-19} C). The electric charge of larger particles, such as ions or molecules, is an integer multiple of the elementary charge. Particles with charges with the same sign repel one another, whereas opposite sign charged particles attract. The magnitude of this force is proportional to the product of their charges and the inverse square of the distance between them. It is useful to employ the concept of the electric field (**E**): at a given point the electric field is a vector (i.e. magnitude and direction)[1] that expresses the force that would be exerted on a positive charge of 1 coulomb placed at that point. Each charged particle creates an electric field which is proportional to its charge, inverse to the square of the distance and that points towards, or against, the particle depending on the sign of the charge. The convenience of the electric field concept comes from the fact that at any point the electric field is calculated as the summation of the electric fields created by each one of the charged particles independently.

[1] In this chapter, bold symbols are used to denote vectors; other authors prefer to use a small arrow over the symbol for the same purpose. A vector is a geometric object that has both a magnitude (length) and a direction. It is usually graphically represented by an arrow connecting two points in a bidimensional or a tridimensional space. In physics, vectors are employed to represent physical entities such as forces and flows.

Electric charges also interact with magnetic fields. The velocity and trajectory of moving electric charges are modified by magnetic fields which in turn are modified by the moving electric charges. Moreover, moving electric charges generate magnetic fields and alternating magnetic fields cause electric charges to move. As a matter of fact, electric forces and magnetic forces are both manifestations of the *electromagnetic force*, which is one of the four fundamental forces identified in nature. To some extent, the interactions between magnetic fields and electric fields are present in the electroporation phenomenology. However, in order to understand most of the electroporation concepts presented here it is not necessary to comprehend those interactions. Therefore, for the sake of simplicity, this chapter intentionally skips magnetic fields and their interactions with electric fields.

Voltage (or potential) value in a point A indicates the energy that a unitary electric charge would have in this point compared to the energy that the unitary charge would have in point B. In other words, voltage is defined as a difference in energy values due to the electric field. When the electric field is constant through the trajectory A-B (e.g. in an infinitesimal trajectory) then the voltage equals the electric field times the distance. For that reason the electric field (**E**) units are V/m. The direction of **E** indicates in which direction the maximum drop in voltage is produced and the magnitude of **E** represents the value of this voltage drop. These concepts are probably better understood with graphical illustrations in which voltages are represented as heights (Figure 1).

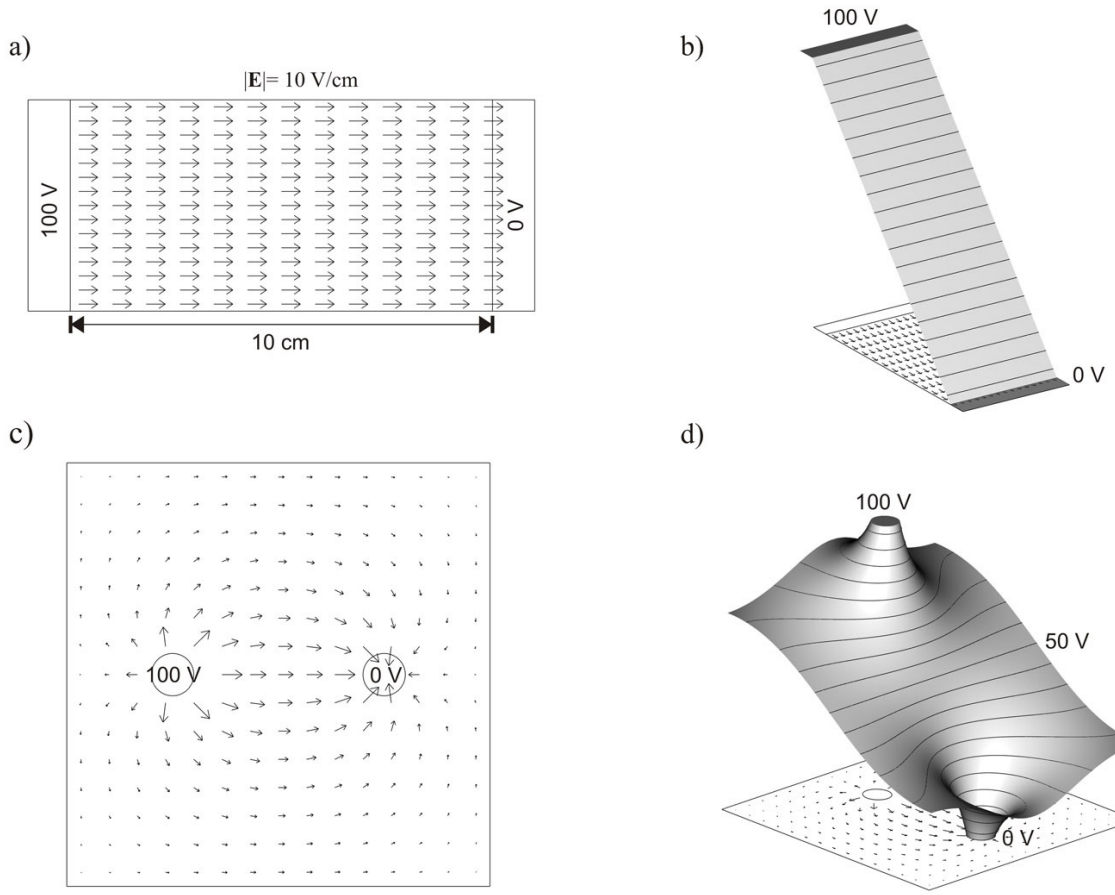

Figure 1. Electric fields and potentials in two bidimensional structures. a) a rectangular slab of homogeneous material with two rectangular electrodes at opposite sides; an electrode is held at 100 V whereas the other is maintained at 0 V; in this case the electric field (represented by arrows) is uniform and its magnitude is equal to the ratio between the voltage difference and the distance (10 V/cm = 1000 V/m), b) voltage values in the previous structure are depicted as height values, c) a square slab of homogeneous material contains two round electrodes, an electrode is held at 100 V whereas the other is maintained at 0 V; in this case the electric field is not uniform, d) voltage values in the previous structure are depicted as height values.

If an electric path exists between two points with different voltages then free electric charges will move from the high energy position to the low energy position. The electric current value indicates the flow of electric charge through the cross-section of the electric path in a second. Traditionally, an analogy with fluidic elements has been displayed in order to explain the voltage and the electric current concepts in circuits: two water tanks at different heights are connected through a pipe and the hydrostatic pressure difference (analogy for the voltage difference) causes the water (analogy for the electrical charge) to flow through the pipe. This analogy is also useful to explain the electrical resistance concept: water flow will not only depend on pressure difference between the tanks but also on pipe diameter and length; the shorter and wider the pipe is, the larger the flow is. A lot of materials exhibit a linear relationship between the electric

current and the voltage difference. This relationship is known as the *Ohm's law* and the constant that relates both parameters is the resistance:

Figure 2. Resistance symbol.

$$V_1 = V_1 - V_2$$

$$R = \frac{V}{I}$$

where R is the resistance (units: ohms, Ω), V is the voltage difference (units: volts, V) and I is the current that flows through the resistance (units: amperes, A). The inverse of the resistance (G = 1/R = I/V) is called conductance and is expressed in siemens, S.

It is important to note that power is dissipated as heat at any conductor. This phenomenon is known as *Joule heating* and it is also referred to as *ohmic heating* or *resistive heating* because of its relationship with the Ohm's law:

$$P_{dissipated} = VI = I^2 R = \frac{V^2}{R} = V^2 G$$

The above definitions for the resistance and the electric current are intended for two terminal components embedded in a circuit. In the case of tridimensional domains it is possible to define equivalent parameters at infinitesimal portions. First it is possible to define the concept of current density (**J**, units: A/m^2) which is the electric current per unit area of cross section. Note that the symbol for current density, **J**, is bolded in order to show that current density is defined as a vector (length indicates magnitude and vector direction indicate direction and sense of the current). Then, it is also possible to define the "resistance" of each infinitesimal portion of a conductive medium: the resistivity (ρ; "rho") of a material at a specific point can be formally defined as:

$$\rho = \frac{\mathbf{E}}{\mathbf{J}}$$

and this expression is completely equivalent to the Ohm's law introduced above.

For a homogeneous material the resistivity can also be defined as:

$$\rho = R\frac{S}{L}$$

where R is the resistance that a cylinder of the material (S is the cross-sectional area of cylinder and L is its length) exhibits between its opposite flat surfaces. Therefore, the units for the resistivity are Ω.m (= $\Omega.m^2/m$). The inverse of the resistivity is the conductivity ($\sigma = 1/\rho$) and it is expressed in S/m (siemens/meter).

The dissipated power due to Joule heating at unitary volume, that is, the dissipated power density (units are watts/cubic meter), can now be written[2]:

$$p_{dissipated} = \frac{|\mathbf{E}|^2}{\rho} = \sigma|\mathbf{E}|^2$$

Here an example can be useful to illustrate the significance of the Joule heating: if a pulse of 1000 V/cm (100,000 V/m) is applied to a living tissue, the maximum possible dissipated power density that will be produced will be about 15×10^9 W/m^3 since the maximum conductivity for tissues is about 1.5 S/m. If the pulse is 100 microseconds (μs) long, then the dissipated energy density (energy = U = power × time) will be 1.5×10^6 J/m^3 (joules/cubic meter). If we assume that the thermal properties of the tissue are equal to those of liquid water and that no heat is lost by radiation, diffusion or convection, which is the worst plausible scenario, then the temperature rise (ΔT) due to the pulse would be:

$$\Delta T = \frac{U}{c\,d} = 0.36\ K$$

where c is the specific heat capacity (c_{water} = 4.184 J/(g.K), joules/(grams × kelvin)) and d is the mass density ($d_{water} = 0.997\times10^6$ g/m^3). Therefore, although the pulse can produce a measurable temperature increase of 0.36 degrees Celsius (°C), it does not seem likely that such ΔT could produce any effect on the viability of the tissues. On the other hand, it is perfectly plausible that some electroporation protocols with multiple pulses (or longer or larger than the 100 μs 1000 V/cm pulse) could result in thermal damage to the tissues. This issue has been addressed in detail by some researchers in the field [12-16] and the main conclusion from those studies is that electroporation, even when it is irreversible, is not necessarily accompanied by thermal damage in the treated region. Nevertheless, thermal damage can appear in specific regions where the electric field is too large, for instance, at the edges of the electrodes. This is an issue to keep in mind when assaying new applications, protocols or electrode setups[3].

[2] |**E**| indicates **E** magnitude; direction is not relevant.

[3] This topic is covered in detail in another chapter of this book by J. Edd, R. Davalos and P. Garcia.

All the electrical concepts presented above were referred to conductive materials and continuous signals. It is convenient now to explain different notions regarding dielectrics and time dependant signals (e.g. alternating voltages).

Dielectrics (i.e. electrical insulators) are materials that are not able to conduct charge. On the other hand, dielectrics support charge accumulation. The physical principles that explain such feature are beyond the scope of this section. Yet it is necessary to introduce here the concept of capacitance. A capacitance is a circuit element able to store, and to release, electric charge. It is created by the combination of conductors and dielectrics. One of its most basic implementations consists of two conductive plates separated by a dielectric material. The amount of charge (Q) that this structure is able to store is determined by its dimensions and by a fundamental parameter of the dielectric: the permittivity (ε, units: C/V.m). Charge stored in the capacitance, at any time, is:

$$Q = C\,V$$

where C (not to be confused with the unit for charge, coulombs) is the capacitance value (units: farads, F). For the conductor-dielectric-conductor structure (Figure 3) the value of the capacitance is:

$$C = \varepsilon \frac{A}{d} = \varepsilon_r \varepsilon_0 \frac{A}{d}$$

where ε_0 is the permittivity of vacuum (= 8.9×10^{-12} C/V.m), ε_r is the relative permittivity of the material ($\varepsilon_r = \varepsilon / \varepsilon_0$), A is the area of the plates and d is the distance between the plates.

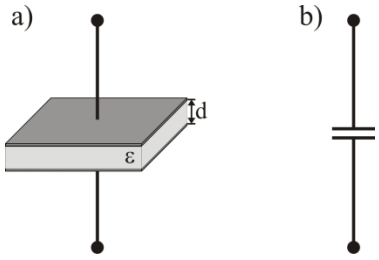

Figure 3. Capacitance. a) simple implementation based on two conductive plates and a dielectric. b) Electrical symbol for a capacitance.

An interesting feature of the capacitance is that it can conduct *displacement currents*:

$$\frac{dQ}{dt} = C\frac{dV}{dt}$$

$$\Downarrow$$

$$I = C\frac{dV}{dt}$$

that is, since the time derivative of the stored or released charge (I=dQ/dt) depends on the time derivative of the voltage, a capacitance acts as a conducting element for fast changing currents. Actual charges do not flow through the capacitance but current appears to do so (i.e. *displacement currents*). Examples of fast changing currents are alternating currents (AC), which are currents whose direction reverses cyclically with a specific frequency. For an alternating signal (voltage or current), it can be said that a capacitance behaves similarly to a resistance with a value that depends on the frequency of the signal. The "resistance" of a capacitance (actually its impedance magnitude or modulus[4]) is:

$$"R_{CAPACITANCE}" = |\mathbf{Z_C}| = \frac{1}{2\pi fC}$$

where C is the capacitance value, f is the frequency of the alternating signal and π is the mathematical constant pi. Note that for high frequencies a capacitance will act as a short circuit whereas for low frequencies it will act as an open circuit.

In all practical cases, capacitances are accompanied by resistances in series. The following example (Figure 4) shows what happens when a voltage pulse is applied to a circuit that consists of a resistance in series with a capacitance (*RC circuit*).

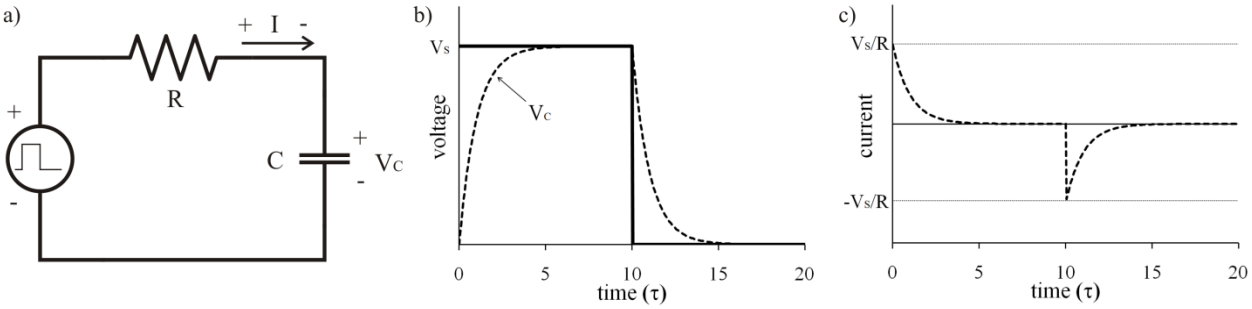

Figure 4. Voltages (b) and currents (c) in a RC circuit (a) when a single rectangular voltage pulse is applied.

At the beginning the capacitance is discharged (Q= 0 coulombs) and, consequently, the voltage difference between its terminals is 0 V. The applied voltage pulse (continuous line) causes current to flow through the resistance and starts to charge the capacitance so that the capacitance voltage (dashed line) increases and the current decreases (voltage difference at resistance

[4] Impedance is a common term in electronics. Usually, it is simply described as the opposition to the flow of an alternating electric current through an electric element or system. Therefore in this sense it is equivalent to a resistance. However, impedance is a broader concept that includes the *phase shift* (delay measured in parts of cycle) between the voltage and the current signals. Impedance is graphically represented with a bidimensional vector whose length represents the magnitude and whose angle represents the phase shift. For mathematical convenience, impedance values are represented with complex numbers.

terminals drops). After a while ($5\tau = 5RC$ [5]) the capacitance is completely charged and almost no current flows through the circuit because the voltage difference at the resistance terminals is null. Then, when the voltage source comes back to 0 V, the capacitance starts to return the accumulated charge through the resistance and the voltage at the capacitance terminals drops slowly down to 0 V. Both, charging and discharging capacitance voltages follow exponential functions:

$$V_C(t) = V_S\left(1 - e^{-(t-t_0)/\tau}\right) \qquad \text{(charging)}$$

$$V_C(t) = V_S\left(e^{-(t-t_0)/\tau}\right) \qquad \text{(discharging)}$$

where V_S is the amplitude of the applied pulse and t_0 is the time at which the charging or discharging starts (in the above example $t_{0\_charging} = 0$, $t_{0\_discharging} = 10\tau$).

3. Cells and tissues in electrical terms

The electrical model that Fricke used in the 20s [1] is still considered to be a good approximation of the passive electrical properties of a single cell for frequencies up to several megahertz. In this model every infinitesimal portion of the extracellular and intracellular media is modeled as a resistance and every infinitesimal portion of the membrane is modeled as a capacitance. Circuit theory allows all those elements to be combined to form a simple equivalent circuit as seen from the electrodes (Figure 5): a resistance representing the extracellular medium (R_e) in parallel with the series combination of a capacitance (C_m), which represents the membrane, and another resistance which represents the intracellular medium (R_i). In a tissue or cell suspension the impedance contribution from all cells is combined so that the same electrical model (obviously with different values) can be employed to characterize the impedance behavior as seen from the measurement electrodes.

[5] The product RC (resistance × capacitance) has units of time and is known as the time constant, τ. In a "RC circuit" it is considered that stable voltages and currents are reached after 5τ.

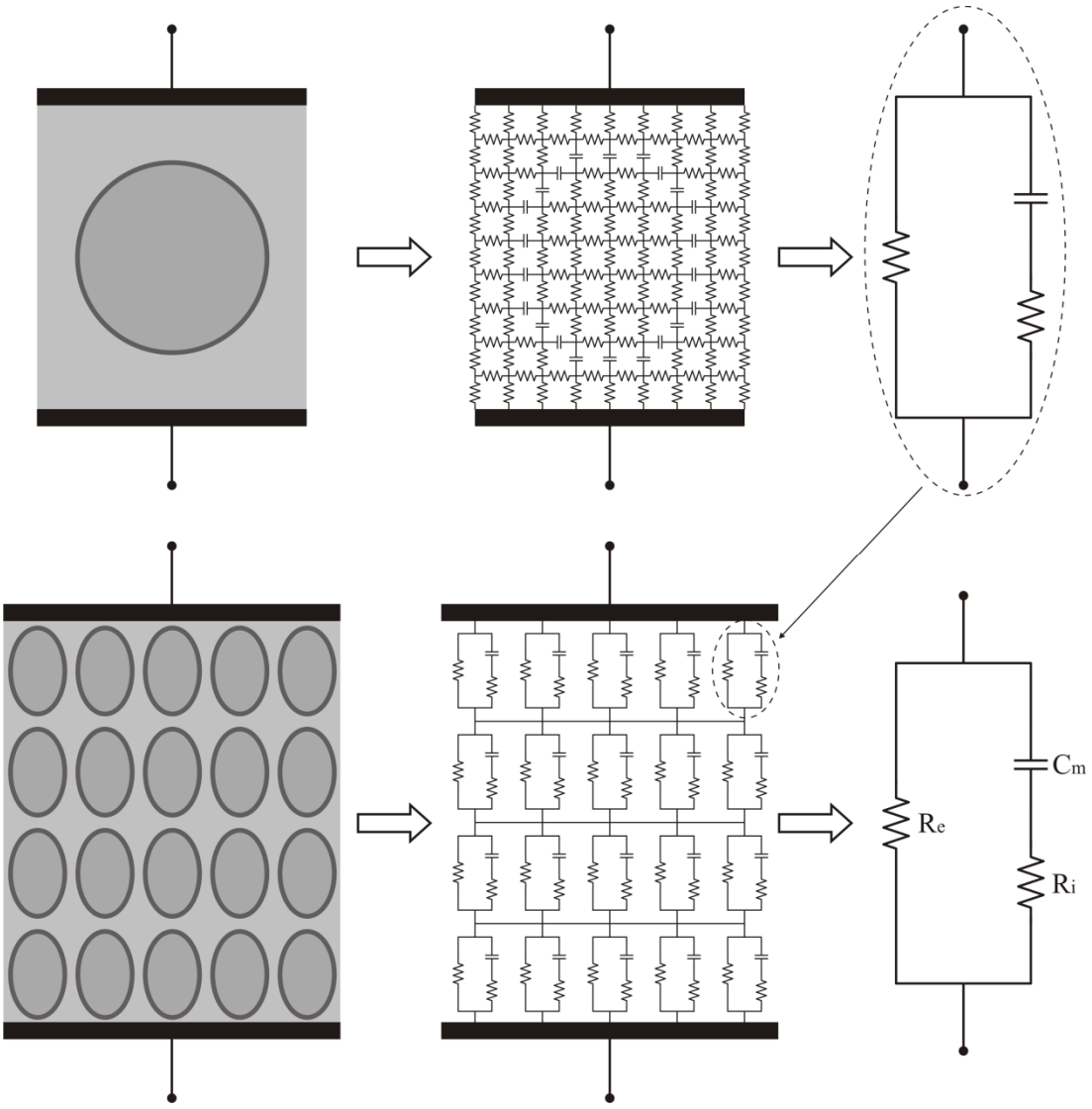

Figure 5. Electrical models for cell (top) and tissue (bottom) as seen from the electrodes. Infinitesimal portions of the extracellular and intracellular media are modeled as resistances and infinitesimal portions of the membrane are modeled as capacitances. All those elements can be combined in an *extracellular resistance* (R_e) in parallel with the series combination of a *membrane capacitance* (C_m) and an *intracellular resistance* (R_i). The same three-element model can be employed to represent the behavior of tissues.

The resistive behavior of the extracellular and intracellular media is basically due to their contents of ions; both media are in fact ionic solutions. Most abundant ions in the extracellular medium are Na^+ and Cl^- whereas in the intracellular media K^+ is the most abundant ion. Blood plasma conductivity at 37 °C is 1.5 S/m (resistivity = 0.66 Ω.m). This is the value that most researchers chose for representing the extracellular conductivity. In some cases this same value is also employed for the intracellular conductivity, although most researchers prefer significantly lower values around 0.6 S/m [17].

The cell membrane consists primarily of a thin lipid bilayer. This film (~ 7 nm thick) is partially permeable to lipids and water molecules to pass through but it is almost impermeable to ions. Its intrinsic electrical conductance is very low and can be considered as a good dielectric. Therefore, the structure formed by the extracellular medium, the lipid bilayer and the intracellular medium is a conductor-dielectric-conductor and it behaves as a capacitance. Experimentally it has been found that such capacitance has a value of about 0.01 F/m^2.

Now, taking into account what has been learnt in the previous subsection about capacitance behavior in the frequency domain (i.e. it behaves as an open circuit at low frequencies and as a short-circuit at high frequencies) it can be understood that low frequency currents will not penetrate into the cell whereas high frequency currents will flow freely through it (figure 6.a). Hence the impedance magnitude (i.e. opposition to current flow) will be higher at lower frequencies (i.e. $|\mathbf{Z}|=R_e$) than at higher frequencies (i.e. $|\mathbf{Z}|= R_e//R_i$) because the electrical paths at low frequencies are narrower[6]. For intermediate frequencies a transitional behavior is manifested (figure 6.b). Typically, for most animal tissues, the transition between the low frequency behavior and the high frequency behavior occurs at frequency band from about 10 kHz to about 1 MHz.

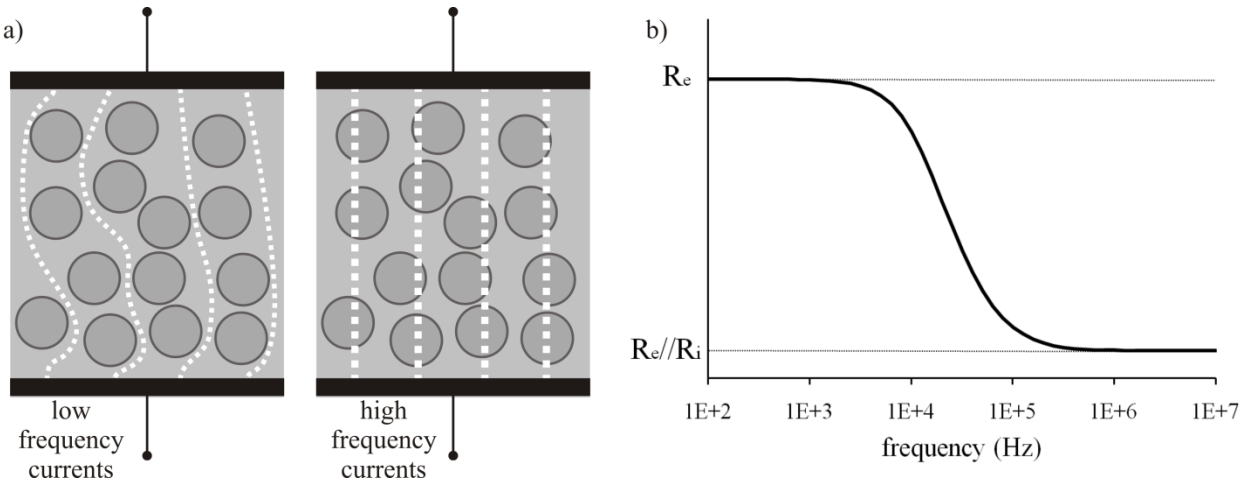

Figure 6. Low frequency currents are restricted to extracellular spaces whereas high frequency currents can flow freely through living tissues. a) Graphic representation of the passage of low frequency and high frequency currents through a cell suspension or tissue. b) Idealized graph of impedance magnitude versus frequency in a living tissue. Note that the scale for the frequency is logarithmic. $R_e//R_i$ represents the value that results from the parallel combination of R_e and R_i which is equal to $R_eR_i /(R_e + R_i)$.

In the time domain the capacitance behavior can also be noticed: when a voltage pulse is applied to a tissue, a peak in current is observed while the cell membranes are being charged; similarly to

[6] Instead of $R_e//R_i$ (i.e. the parallel combination of R_e and R_i), the impedance magnitude at high frequencies is also denoted as R_∞ (where ∞ indicates infinite frequency) and instead of using R_e it is noted R_0 to indicate the impedance magnitude at low frequencies (ideally 0 Hz).

what is depicted in figure 4.c. The duration of the peak (i.e. membrane charging process) is typically in the order of a fraction or a few microseconds.

Embedded within the lipid bilayer there are different sorts of protein structures that play a fundamental role in cell activities (e.g. transportation of substances across the membrane, inter-cell communication and surface recognition). Of particular relevance here are the ionic channels which are porous structures that allow some ions to flow through the membrane. These structures are selective to specific ions and can be opened or closed depending on different parameters such as the *transmembrane potential*[7]. Hence the electrical model displayed in figure 6 needs to be modified slightly in order to include the short-circuiting effect caused by these structures. In other words, the cell membrane is not a perfect dielectric and some leakage current through it can exist (Figure 7).

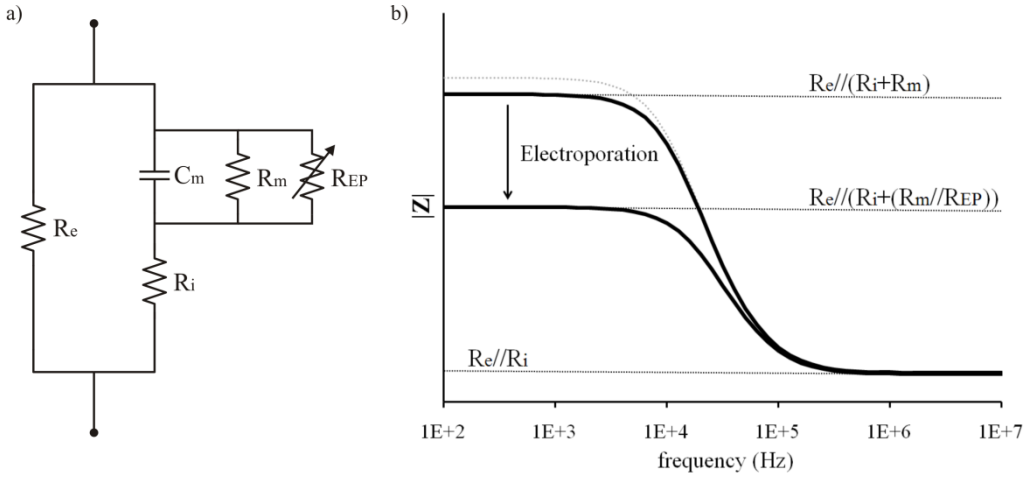

Figure 7. The cell membrane is not purely dielectric, it has some residual conductivity that is increased by the electroporation phenomenon. a) Enhanced electrical model for a living tissue: R_m represents the short-circuiting resistance across the membrane due to ionic channels and R_{EP} represents the increased conductance due to the electroporation phenomenon (the arrow denotes that it is variable). b) Graph of impedance magnitude versus frequency for the enhanced electrical model. The impedance magnitude at low frequencies is slightly lower than R_e (figure 6.c). Electroporation causes a significant drop in impedance magnitude at low frequencies.

When electroporation occurs, cell membrane becomes more permeable and, therefore, the cell conductance (i.e. the inverse of the cell resistance) increases. At high frequencies this effect is not manifested in the impedance magnitude but at low frequencies a significant impedance magnitude drop can be observed. This issue will be covered in more detail in subsection 6.

[7] The *transmembrane potential*, or *transmembrane potential* or, simply, *membrane voltage*, is the voltage difference between the interior and the exterior of the cell.

All what has been said above refers to the linear[8] passive electrical properties of biological samples. These properties are usually grouped with the term *bioimpedance*. The bioimpedance model described here is the simplest one for cells and tissues. Such model is appropriate to understand the electroporation phenomenon but it must be said that current bioimpedance knowledge is significantly more complicated. Readers interested in this topic will find further details in [18] or [19].

Cells also exhibit non-linear and active electrical properties. Nerve and muscle cell membranes contain specific ion channels that make them electrically excitable: an adequate disturbance of the transmembrane resting potential will trigger a sequence of fast changes in the membrane permeability to specific ions known as an *action potential* (AP). The AP in a spot of the membrane will affect adjacent portions of the membrane and will propagate as a voltage impulse through the nerve or the muscle fiber. This is the basic mechanism that allows *nerve impulses* (actually another name for AP) to propagate through the axons of afferent (i.e. sensory) nerves or efferent (i.e. motor) nerves. This also explains how the contraction wave is propagated through the myocardium so that the heart performs its pumping action.

AP propagation can be considered as a non-linear passive phenomenon. However, it depends to a large extent on the existence of a transmembrane resting potential. This resting potential between the interior and the exterior of the cell (approximately -70 mV for neurons) is kept constant thanks to an active mechanism in which specific ions are pumped inside and outside of the cell. Action potentials can be initiated when the resting transmembrane is cancelled or surpassed (i.e. *membrane depolarization*) by the application of an external electrical stimulus.

Additional knowledge on AP generation and its propagation may be convenient to fully comprehend subsection 7 in this chapter, however, no further details are included here because there is a large variety of sources that explain those topics from a natural sciences perspective, without assuming a strong background in electromagnetism; textbooks on cell physiology and human physiology are probably proper choices for most readers.

4. Electroporation threshold

There are numerous evidences from experiments on cell suspensions [7, 20, 21], on isolated cells [4, 22, 23] and on artificial membranes [24-26] that electroporation occurs when the transmembrane voltage reaches a specific threshold. The value of such threshold depends on the characteristics of the applied pulses (number, duration and shape) and also on how electroporation is assessed (e.g. by noticing an increase of membrane conductance, by detecting

[8] The word *linear* in this context implies that these properties have the same value regardless of the magnitude of the test signal. When certain stimulus thresholds are surpassed, those properties are not linear anymore.

intracellular contents release or by observing cell lysis). Most authors report threshold values in the range from 200 mV to 1 V.

When an electric field is applied to a biological sample (e.g. a cell suspension or a tissue), after a short delay[9], transmembrane voltages are induced on the cells membranes. If the magnitude of the field is large enough, the induced transmembrane potentials will cause electroporation.

Before electroporation occurs, or for low electric field magnitudes, the induced transmembrane voltages are proportional to the magnitude of the applied field[10]. In the case that a uniform field is applied to a single cell in suspension, or to a diluted suspension[11], it is possible to employ a simple model in order to predict when electroporation will occur: for a spherical cell of radius r with negligible membrane conductivity (Figure 8) the induced transmembrane potential (ΔV_m) at each membrane point is [22]:

$$\Delta V_m = \frac{3}{2}|\mathbf{E_{ext}}|\, r\cos(\theta)$$

where θ is the angle between the radius (from cell center to evaluation point) and the applied external field ($\mathbf{E_{ext}}$). This expression is sometimes referred to as the *Schwan's equation* [28].

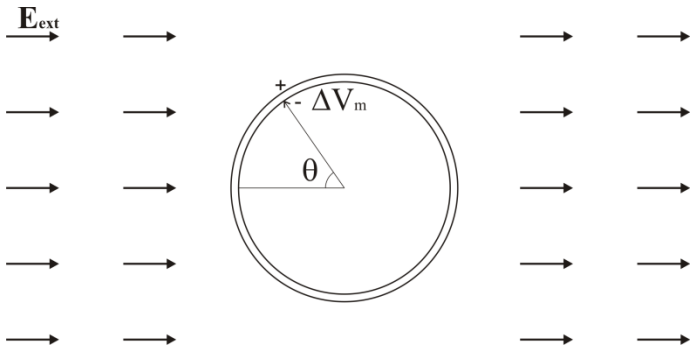

Figure 8. An external electric ($\mathbf{E_{ext}}$) field induces a modification of the transmembrane potential. The electric field is intentionally not drawn in the vicinity of the cell because there it is not uniform (see Figure 9).

[9] This delay is due to the cell membrane charging process. See the next section 5.

[10] When electroporation occurs the conductance of the membrane changes abruptly and the relationship between the electric field magnitude and the transmembrane voltage is not linear anymore (this is analyzed in the next section 5). Actually, the cell membrane behavior can be nonlinear before reaching the electroporation threshold; some of the ion channels are voltage gated and they will switch at low transmembrane voltages. Nevertheless, for the sake of simplicity, this voltage gating phenomenon is ignored by most researchers working on electroporation models.

[11] According to [27] this model is valid when the volume percentage occupied by the cells is lower than 0.6%. For larger fractions the same paper gives an expression to correct the predicted transmembrane voltage values.

Therefore, since ΔV_m is proportional to the cell radius, lower fields will be required to achieve electroporation in larger cells. This fact has significant consequences when cell suspensions are electroporated in a cuvette[12]. For instance, the magnitude of the applied electric field needs to be optimized for each cell type and better results will be obtained for cell lines with small variations in cell sizes. On the other hand, in some cases it may be interesting to electroporate selectively the large cells in a heterogeneous sample [30].

Another interesting consequence of the above equation is that electroporation will not occur uniformly across the cell membrane; some areas will be easily electroporated (i.e. large $|\Delta V_m|$) whereas other will remain intact ($|\Delta V_m| \sim 0$ V). In particular, cell areas facing the electrodes, that is, perpendicular to the field direction ($\theta \sim 0$) will experience larger transmembrane voltages and therefore will become more easily electroporated. This phenomenon is nicely illustrated in [23]. In that paper, the researchers employed voltage-sensitive fluorescence dyes combined with fast microscopy and they were able to observe that 1) large $|\Delta V_m|$ occurred at the cell poles facing the electrodes and 2) at those areas it was observed a huge increase in membrane conductivity (i.e. electroporation). In a more recent paper by the same research group [31], the effect of the resting transmembrane potential is discussed: since this physiological potential (approximately +70 mV as defined[13] in figure 8) is added to the transmembrane voltage change induced by the external field, the cell pole facing the positive electrode (i.e. the anode, that is, left side in figure 8) reaches the transmembrane voltage threshold required for electroporation before it does the negative pole. This interesting observation, however, has little practical impact on electroporation since the induced transmembrane voltages will be typically much larger than the resting potential (e.g. 500 mV against 70 mV), particularly in irreversible electroporation.

For more complex geometries than that shown in figure 8 the equations that describe the induced transmembrane potential are much more intricate or do not exist. For those cases it is convenient to make use of numerical methods implemented on computers. For instance, in [32] the *finite element method* was employed to conclude that the maximum transmembrane potential induced in erythrocytes (biconcave shape) must be 22 % lower than the maximum transmembrane potential that is reached in an spherical cell of the same size.

There are different numerical methods for calculating physical variables in scenarios with arbitrary geometries. One of those methods suitable for computer simulations is the *finite element method* (FEM). The key idea of the FEM is the decomposition of the geometry into small simple elements (i.e. the *mesh* of elements) in which it is possible to solve differential equations related to the phenomenon under study. Boundary conditions impose the constraints

[12] This electroporation method has been employed for more than 20 years in microbiology labs after the design by Potter et al. [29] .

[13] In neurophysiology this potential is represented with negative sign because the potential is defined between the interior and the exterior of the cell, and not between the exterior and the interior of the cell as it is the case here.

that allow the method to generate a single approximate solution for the complete geometry. Up to a point, FEM is equivalent to the decomposition in a matrix of simple elements shown in figure 5.

Figure 9 displays results from tridimensional FEM simulations of the induced transmembrane potential for different modeled cells under an external uniform field of 1000 V/cm (100 kV/m). The first three cases (a, b and c) correspond to the spherical cell model depicted in figure 8 and show the two main features that were expected from the above equation: 1) induced transmembrane potential is proportional to cell size and 2) transmembrane potential is not uniform across the cell membrane; the poles facing the electrodes experience a larger voltage. As matter of fact, the cell poles in the subfigure b (radius = 5 μm) reach the transmembrane voltage predicted by the equation, that is, 750 mV. The last three cases (d, e and f) correspond to an ellipsoidal cell (20 μm × 10 μm × 10 μm) that is oriented in different directions relative to the electric field. Although it is not easily observable in the figure, in the parallel orientation higher voltages are reached. Therefore, a general rule that can be intuited from these results is that induced transmembrane potentials depend on cell size, cell shape and cell orientation. It is s worth noting that a recent paper by Towhidi et al. [33] reports magnificently a experimental study in which multiple cells exhibit different electroporation thresholds depending on their sizes, shapes and orientations.

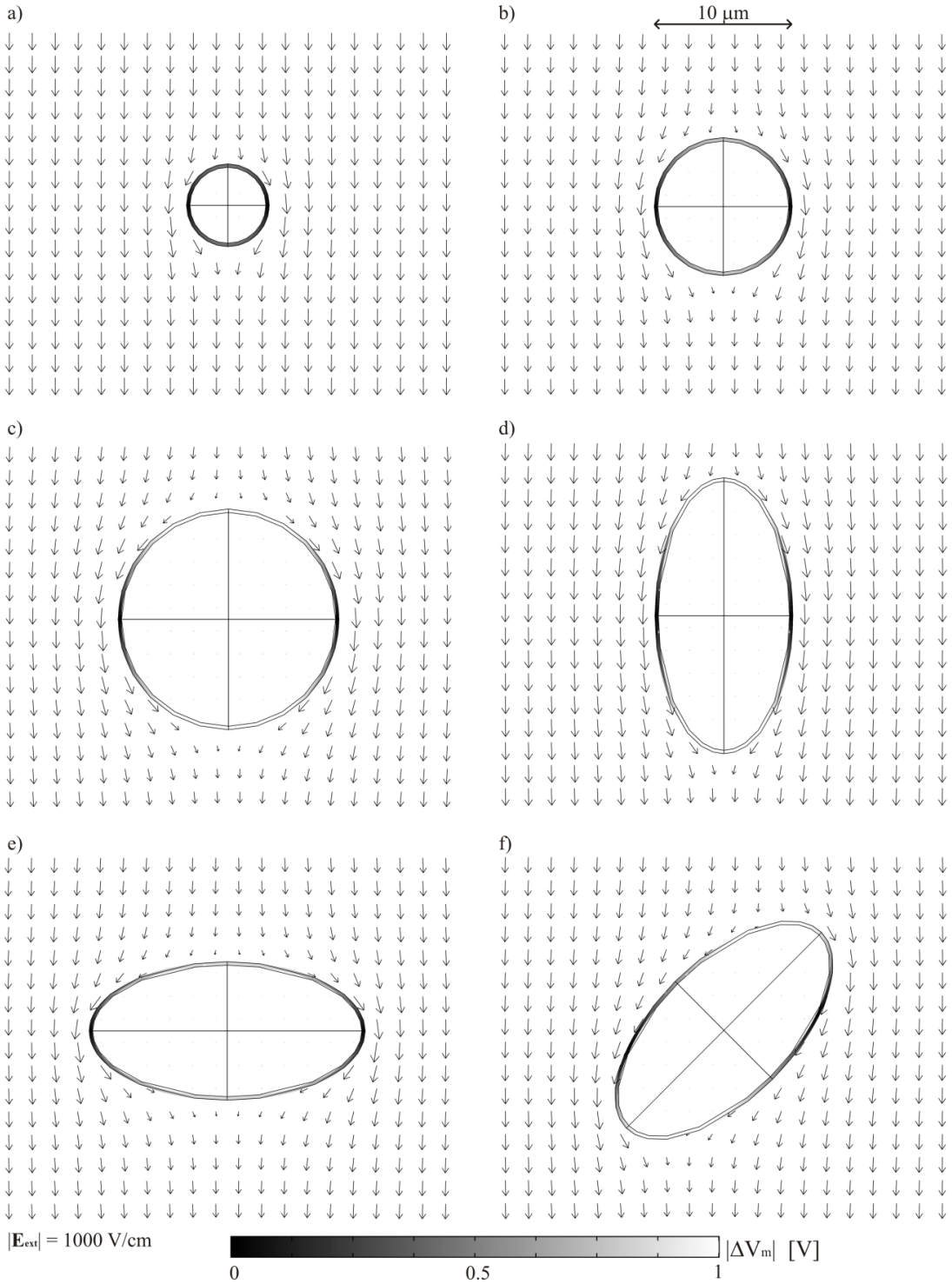

Figure 9. Tridimensional FEM simulations of the transmembrane potential induced by an external electric field of 100 kV/m. Only a single plane (across the center) is shown for each cell case. Arrows indicate field magnitude and direction. a) Spherical cell of 6 microns in diameter: no membrane region is above 0.5 V .b) Spherical cell of 10 µm in diameter: top and bottom poles reach 0.75 V (in absolute value). c) Spherical cell of 16 µm in diameter: large regions are above 1 V. d) Ellipsoidal cell (20 µm, 10 µm, 10 µm) parallel to the field direction. e) Ellipsoidal cell (20 µm, 10 µm, 10 µm) perpendicular to the field direction. f) Ellipsoidal cell (20 µm, 10 µm, 10 µm) oblique to the field direction.

Notice in the simulations displayed in figure 9 that the electric field is significantly distorted in the vicinity of cells. This fact implies that in dense cell suspensions and tissues, where the spaces between cells are narrow, the electric field will be far from uniform at microscopic level. Hence the above equation for the induced transmembrane voltage in the case of an isolated cell will be useless for tissues. However, given that the resistivity of some tissues can be assumed to be homogeneous at macroscopic level, it is possible to consider a *macroscopic* electric field distribution. Then it is reasonable to hypothesize that cells in a specific tissue region will be electroporated if the macroscopic electric field magnitude at that region reaches or surpasses a specific field magnitude threshold. Such threshold will not only be dependent on electroporation parameters but also on tissue type, similarly to what happens with suspensions of cells of different lines. Besides cell sizes, shapes and orientations, here the intercellular distances will also play a significant role. That is, the separation between cells will modulate the transmembrane potential induced by the external macroscopic field [34].

The above hypothesis is now commonly employed to predict the extension and shape of tissue volume that will be electroporated with a specific electrode setup. Figure 10 illustrates how this is done. It is first created a geometrical model of the tissues and the electrodes in which tissues conductivities are modeled as being homogeneous (in Figure 10 a single tissue type is modeled). Then the electric field distribution is computed by analytical or computer assisted methods[14]. And, finally, it is considered that only the cells at areas where the field magnitude surpasses a specific threshold reach a sufficiently high transmembrane voltage for successful treatment. This sort of *treatment planning* has been validated in multiple experimental studies [36-39].

[14] In some simple cases it is possible to find analytical solutions (i.e. equations) that describe the field distribution [35], however, in most cases computer tools based on numerical methods such as FEM will be necessary.

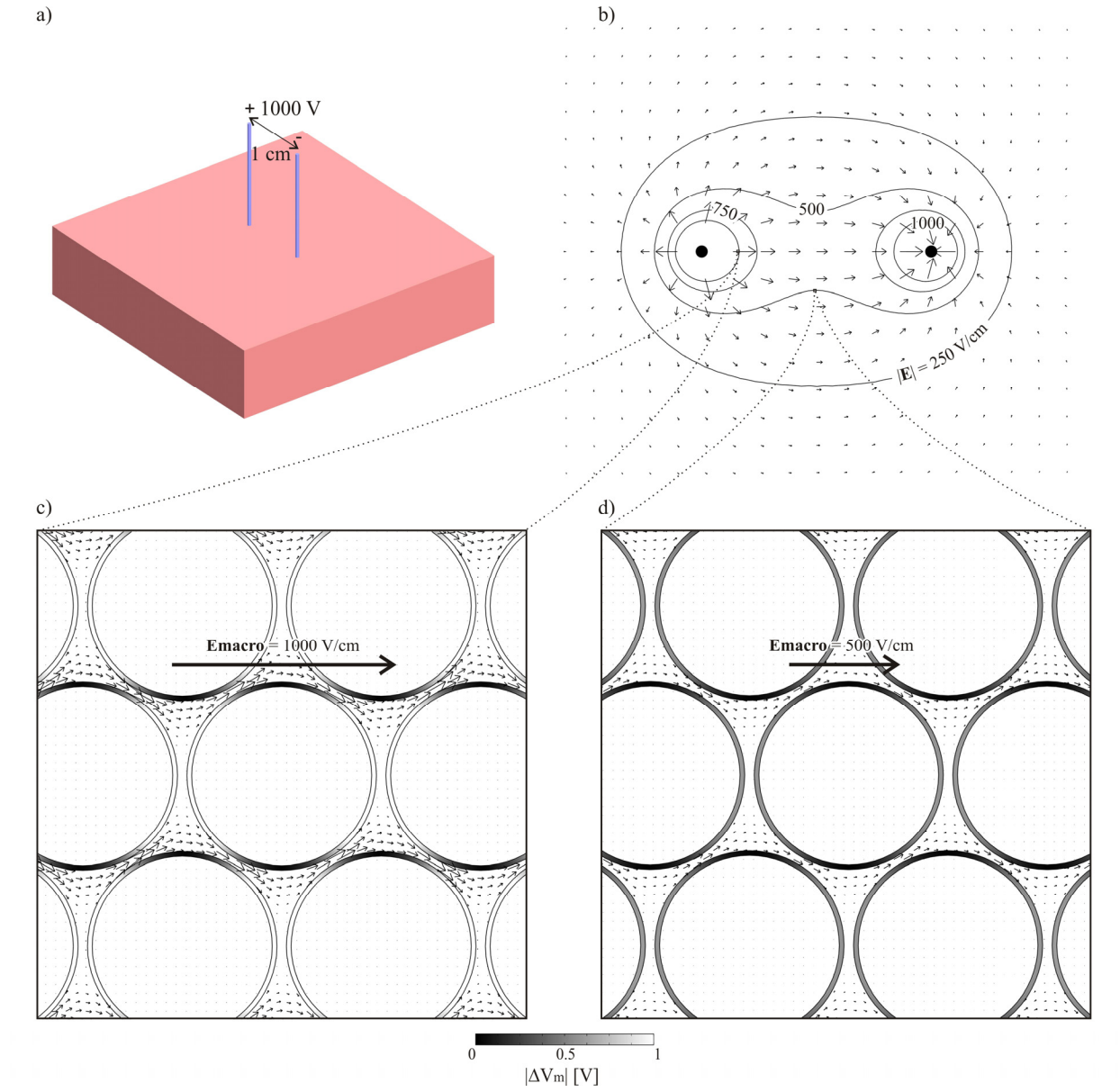

Figure 10. The electric field distribution is computed by FEM under the assumption of a tissue with homogeneous conductivity. a) Geometrical model employed in this example: two needle electrodes of 0.5 mm in diameter are inserted into the tissue at a separation distance of 1 cm and 1000 V are applied between the electrodes. b) The simulated electric field (arrows) is displayed at the tissue surface; four isolines of the electric field magnitude are also displayed (250, 500, 750 and 1000 V/cm). c) Induced transmembrane potentials (ΔV_m) in a hypothetical tissue (packed round cells with a diameter of 20 µm) located at an area where the magnitude of the macroscopic field is 1000 V/cm. d) The same as subfigure (c) but at an area where the field magnitude is 500 V/cm. Note: the length scale for the microscopic field distribution in subfigures (c) and (d) is not the same than the one use for the macroscopic field.

At least three different electric field thresholds can be defined that are of interest in electroporation. The lowest of them would be the threshold for the manifestation of reversible electroporation (E_{rev}); only the cells within areas where $E \geq E_{rev}$ are electroporated. If a second

threshold (E_{irrev}) is reached or surpassed, electroporation will compromise the viability of the cells. A larger threshold can also be defined ($E_{thermal}$) for the manifestation of thermal damage caused by the Joule effect. This is particularly relevant in the case of IRE ablation techniques: if irreversibility threshold is surpassed but thermal threshold is not reached then cells are destroyed but tissue scaffold is spared and that facilitates post-treatment healing [40].

Therefore, the goal of simulations in electroporation treatment planning must be to guarantee that a rather homogeneous electric field magnitude ($E_{min} \leq E < E_{max}$) is created in the region of interest and that an electric field magnitude as low as possible is induced in the regions not to be treated. Note that here it has been indicated that the electric field magnitude in the region of interest must be between E_{min} and E_{max} instead of E_{rev} and E_{irrev} or E_{irrev} and $E_{thermal}$. The E_{rev} and E_{irrev} labels are usually employed to denote the minimum electric field magnitudes at which reversible electroporation and irreversible electroporation can be manifested, but that does not imply that all the cells will experience reversible or irreversible electroporation. In other words, if the electric field magnitude at a certain area is slightly larger than E_{rev} that does not guarantee that all the cells in that area will experience enough reversible electroporation. Again, multiple factors, such as cell size, cell shape and intercellular spacing, modulate the induced transmembrane voltage. By performing animal and preclinical experiments it is possible to obtain an E_{target} that represents the optimal electric field magnitude for a specific treatment. Then it is also possible to define a tolerance around this value. That is, in the region to be treated, the electric field magnitude must be within this tolerance interval in order to achieve successful treatment.

Up to now, electroporation treatment planning has been focused on designing suitable electric field distributions by choosing: 1) the location, and shape of the electrodes and 2) in some cases, the order and sequence in which high voltage pulses are applied between the involved electrodes. For instance, Gilbert et al.[41] proposed the use of needle structures in which the pulses were applied between opposite electrodes in a rotating sequence. Recently, in [42], we introduced a third mechanism of control for the distribution of the electric field: the use of electrolytic gels and liquids which have specific conductivities so that the field distribution can be modulated. For instance, in the particular case of tissue electroporation by using plate electrodes, a gel with a conductivity similar to that of the tissue can be employed in order to homogenize the field distribution as it is illustrate in figure 11. In [43] we demonstrate *in vivo* the effectiveness of this specific technique and we show that it is tolerant to conductivity mismatching errors between the gel and the tissue.

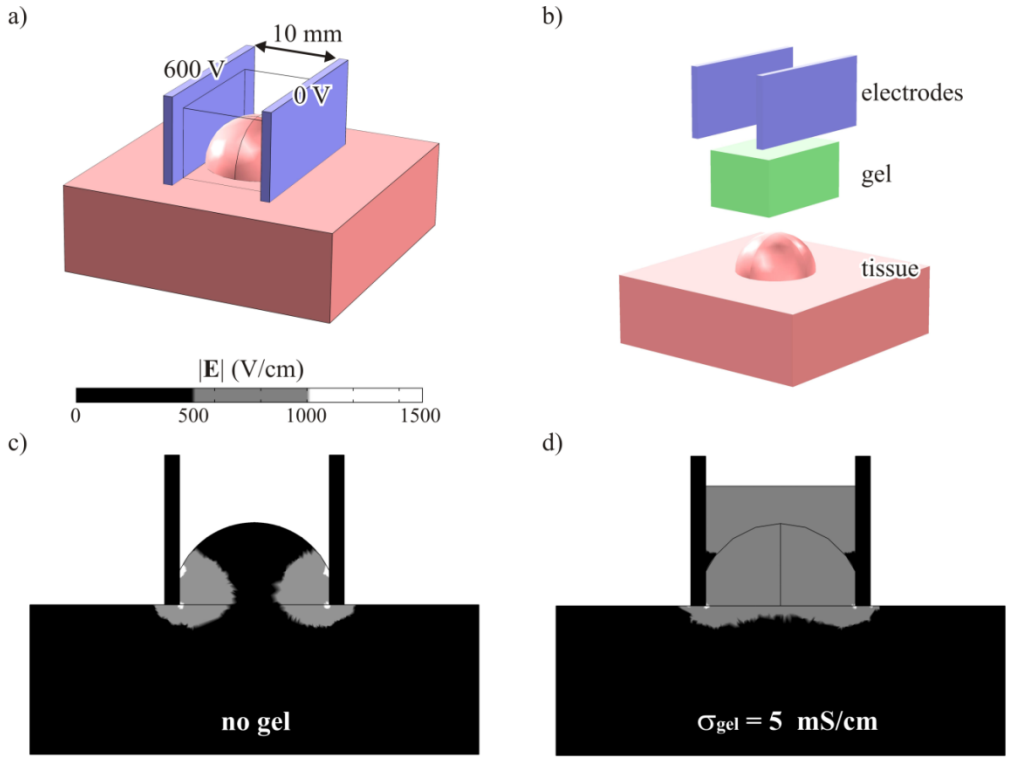

Figure 11. Use of conductive gels, matched to the conductivity of the tissue, to fill dead spaces between plate electrodes gripping the tissue so that the electric field distribution becomes less heterogeneous. a) and b) Geometrical model employed for the simulation. c) Simulation result when no gel is used; the field distribution is too heterogeneous. d) Simulation result when a gel with conductivity of 0.5 S/m is applied. This technique is tolerant to conductivity mismatches between the gel and the tissue [43].

5. Time course of currents and electric fields during electroporation pulses

As it has been mentioned above, due to the membrane charging process there is a delay between the application of the electric field and the materialization of the induced transmembrane voltage. Actually, it is more accurate to say that transmembrane voltage is not delayed but increases slowly up to a stable value. For the spherical cell model of figure 8 it is possible to write the equations that describe such behavior [23]:

$$\Delta V_m = \frac{3}{2}|\mathbf{E_{ext}}|\, r\cos(\theta)\left(1-e^{-t/\tau}\right)$$

$$\tau = r C_m\left(\rho_i + \frac{\rho_e}{2}\right)$$

where C_m is the capacitance of the cell membrane per area unit and ρ_i and ρ_e are the resistivities of the intracellular and the extracellular media respectively.

Therefore, if a very short pulse is applied (duration in the order of τ)[15] the transmembrane voltage will not reach its maximum possible value ($\Delta V_{m\_max}=1.5\times|\mathbf{E_{ext}}|\times r$ at time >> τ) and probably the cell will not experience electroporation unless $|\mathbf{E_{ext}}|$ is extremely high. Another interesting consequence is that larger cells will experience larger transmembrane voltages but they will require more time to reach the stable voltage. At this point it is opportune to mention the research that multiple groups are carrying out regarding the use of very high voltage pulses of very short duration; in the order of some nanoseconds or tens of nanoseconds [44-49]. The main motivation for this research comes from the believe that those ultra-short pulses, known as nanosecond Pulsed Electric Field (nsPEF), could be able to induce electroporation of intracellular membranous structures (e.g. mitochondria) without disturbing the cell membrane. In *conventional* electroporation, that is, with pulses larger than 10 μs, the cell membrane reaches its maximum transmembrane potential and when this happens the intracellular structures become isolated from the external field and hence cannot experience electroporation[16]. On the other hand, it seems reasonable that if very short pulses of high magnitude are applied then the intracellular membranous structures will be charged to a sufficiently high voltage for electroporation before the cell membrane is barely charged. That is the reason why it was expected that it would be possible to electroporate internal structures without causing electroporation of the plasma membrane. However, recent computer models [51] and experimental results [52] indicate that cell membrane electroporation also occurs when nanosecond pulses are applied. That is, with nsPEF all the membranous structures of the cell are electroporated (some authors refer to this phenomenon as *supraelectroporation*). This is illustrated in figure 12: it is simulated the evolution of the transmembrane potential in the cell membrane (ΔV_{m_out}) and in the membrane of an internal structure (ΔV_{m_in}). After two microseconds (subfigure a) the cell membrane potential reaches the predicted stable value ($\Delta V_{m\_max}=1.5\times|\mathbf{E_{ext}}|\times r$) and the potential across the membrane of the internal structure drops to zero. However, during the first nanoseconds after the pulse is applied (subfigure b) both transmembrane potentials are very similar. Hence if a very short electric field pulse is applied (~ 20 ns) and it has a much larger magnitude than the pulse applied in the example, it is reasonable to expect that both membranes will reach a sufficient transmembrane voltage for electroporation.

[15] A round cell of 20 μm in diameter will have a charging time constant, τ, of about 0.18 μs (Cm = 0.01F/m, ρ_e = (1/1.5) Ω.cm, ρ_i =(1/0.66) Ω.cm).

[16] This statement, given by researchers in the nsPEF field [50], is not necessarily true: when the cell membrane transmembrane voltage is large enough to induce electroporation, the membrane resistivity drops dramatically and internal structures are not isolated anymore from the external field. Therefore, if the magnitude of the field is extremely large (as it may be the case in IRE) the smaller internal structures might also be electroporated.

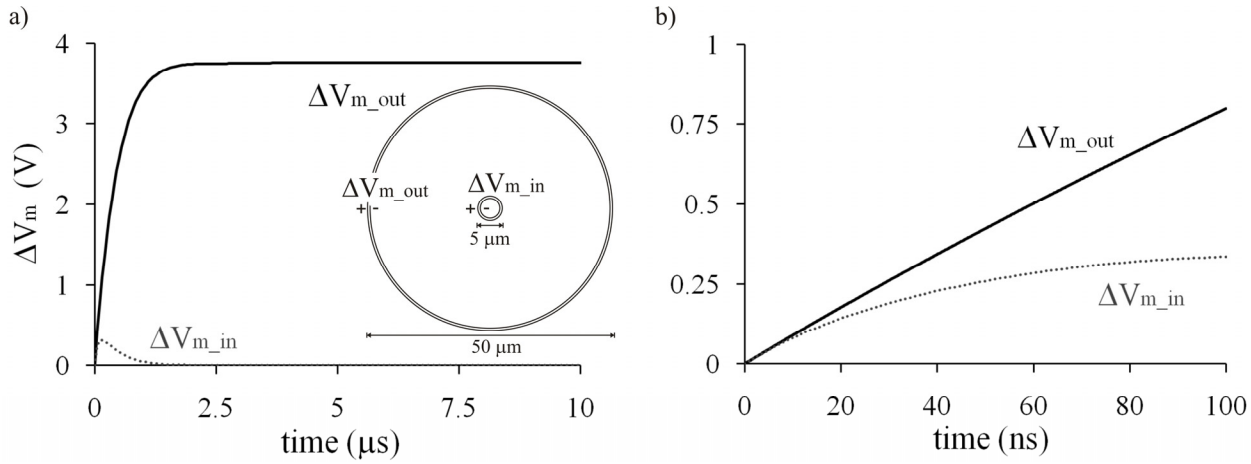

Figure 12. Simulation of the evolution of the transmembrane potential in a cell membrane (ΔV_{m_out}) and in the membrane of an internal structure (ΔV_{m_in}). The magnitude of the applied electric field is 1000 V/cm.

The fact that nanosecond pulses are able to achieve electroporation implies that the electroporation process occurs very rapidly once the transmembrane voltage threshold is reached; in a matter of a few nanoseconds at most. In fact, by performing membrane conductance measurements it was demonstrated more than twenty-five years ago that "membrane breakdown" occurs in less than 10 ns [53].

In all the above equations and examples for the transmembrane potential it has been assumed that the conductivity of the membrane is always extremely low. However, once the transmembrane potential reaches the critical value and electroporation occurs, this assumption is no longer valid and it is easy to understand that the short-circuiting effect caused by the permeabilization will somehow neutralize the transmembrane voltage rise. This is illustrated experimentally in [23]. There it is shown that the $\cos(\theta)$ is not held when the electric field magnitude goes above a certain threshold: the profile of the transmembrane voltage across the membrane flattens at the poles facing the electrodes. That is, the transmembrane potential does not seem to go above a critical value which is only slightly larger than the threshold to initiate electroporation.

In fact, one could expect that the transmembrane voltage would go back to values much lower than the electroporation threshold (imagine the hypothetical case in which the electroporation effect is so intense that the membrane is fully short-circuited; that would imply $\Delta V_m = 0$). And indeed it has been noticed experimentally [31] and it has been predicted by electroporation models [54] that the transmembrane potential can slowly decrease in a matter of a microseconds or tens of microseconds. Nevertheless, a dramatic and sudden drop in transmembrane potential is not observed. The transmembrane potential remains quite stable after the critical value has been reached. This would be an indication that the sort of permeabilization that occurs immediately (in a matter of nanoseconds) is somehow reversible also in an immediate fashion: the

permeabilization tends to reduce the transmembrane voltage but if that happens then the conductivity decreases immediately and hence voltage goes up again, and, therefore, the voltage remains stable. On the other hand, the slow decrease of the voltage that comes later during the pulse would indicate that membrane conductivity is increasing in a way that cannot be reversed immediately after removing the electric field.

To sum up all the above concerning single cell studies: 1) electroporation does not occur until the transmembrane voltage reaches, in about a few microseconds, a critical value (between 200mV and 1V), 2) once it reaches this value the conductivity of the membrane increases immediately (< 10 ns) to a value that keeps the transmembrane voltage close to the critical value and 3) then the membrane conductivity keeps rising slowly during the application of the pulse.

In figure 13 it can be observed a typical behavior of the current signal when a rectangular electroporation pulse is applied to a living tissue or a very dense cell suspension. This example does not correspond to an actual experiment but it shows the main features that can be noticed in actual measurements in tissues [55, 56] or dense cell suspensions [57]: after an initial peak due to cell membrane charging, current increases exponentially and afterwards it seems to increase much slower in a linear fashion or it stops increasing. The initial abrupt change in conductance[17], masked by the membrane charging process, is probably the manifestation of the immediate and reversible membrane permeabilization mentioned before. The later exponential rise shows that membrane conductance increases slowly and moderately during the pulse.

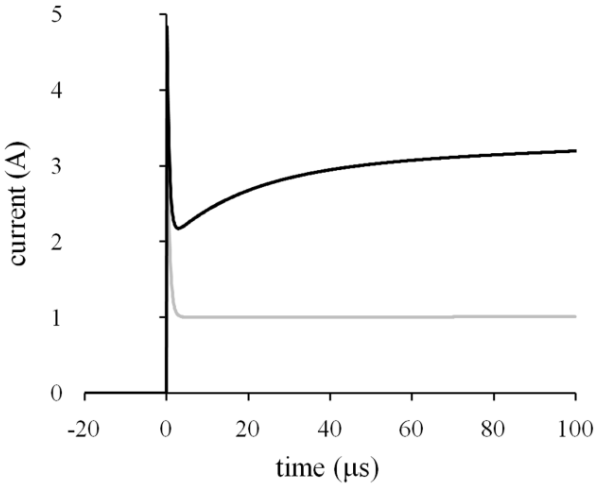

Figure 13. Typical recording (black line) of current during the application of a 100 μs high voltage pulse. The gray line indicates what would be the response if electroporation did not occur: after a peak in current due to cell membrane charging, current would increase very slightly (almost unappreciable in the graph) because of resistive heating.

[17] G=I/V and in this case V is constant, therefore, conductance is directly proportional to the current.

The gray line in figure 13 shows what would be the behavior of the tissue in case the electroporation phenomenon did not exist. After the peak due to the membrane charging process, tissue conductivity would increase moderately, almost inappreciably, due to resistive heating. This tissue conductivity increase due to Joule heating is related to the fact that the conductivity of ionic solutions shows a positive dependence on the temperature. In the particular case of physiological fluids is estimated that the conductivity increases 2% per each °C [58]. In the above example the resulting increase of conductivity due to thermal heating is not significant, however, this phenomenon should be kept in mind as it can be significant in other cases [57].

Following the replacement concept of the 3 Rs approach for animal testing[18], it is convenient to note here that some vegetables can be a proper alternative for studying bioelectrical aspects of tissue electroporation. In particular, raw potato tuber is a good choice because any irreversibly electroporated area will be distinctively darker 5 hours after electroporation[19]. Figure 14 displays the ratio between the conductivity at specific times of a 5 ms pulse (10 μs, 100 μs and 1000 μs) and the original potato conductivity (σ_0); multiple field magnitudes are tried. Observe that the immediate (10 μs) change in conductivity is quite significant (15 times the original conductivity), that it follows an almost linear relationship with the field magnitude up to 400 V/cm and that for larger field values it seems to saturate. During the pulse the conductivity keeps rising, but at a slower pace (values at 5 ms are virtually equal to those at 1 ms), and the maximum conductivity that it is reached is about $30\times\sigma_0$. It is interesting to note that this maximum ratio ($\sigma_p/\sigma_0 = 30$) is really close to the impedance ratio R_0/R_∞ that is measured before electroporation[20]. This is in agreement with the electrical model of electroporation depicted in figure 7: in principle, the minimum resistance that can be reached by electroporation must be equal to the minimum impedance magnitude that can be obtained by applying high frequencies (R_∞); in both cases the cell membrane is "short-circuited". Therefore, at 5 ms, for field magnitudes larger than 400 V/cm, cell membrane has become so permeable to ions that its resistance is insignificant when compared to the resistance of the intracellular and extracellular media. Such statement does not imply that membrane is completely disrupted; only a tiny fraction of the membrane area needs to be opened (<1%) in order to achieve such irrelevance in terms of conductivity [31].

---

[18] The 3Rs approach was introduced by Russell and Burch [59]. The 3 Rs represent: **r**eduction of the number of animals used, **r**efinement of techniques and procedures to reduce pain and distress, and **r**eplacement of animal with non-animal techniques.

[19] When the electroporation protocol consists of 8 pulses of 100 μs at 10 pulses/s then the electric field threshold for irreversible electroporation is about 300 V/cm (not published data obtained by the author; methods equivalent to those in [60]). Potato darkening after 5 hours is probably due to an accelerated oxidation of chemical constituents caused by a decompartmentalization of certain enzymes and substrates [61] that occurs at cell lysis caused by electroporation.

[20] R_0/R_∞ is the ratio between the impedance magnitude at low frequencies and the impedance magnitude at high frequency; see subsection 3.

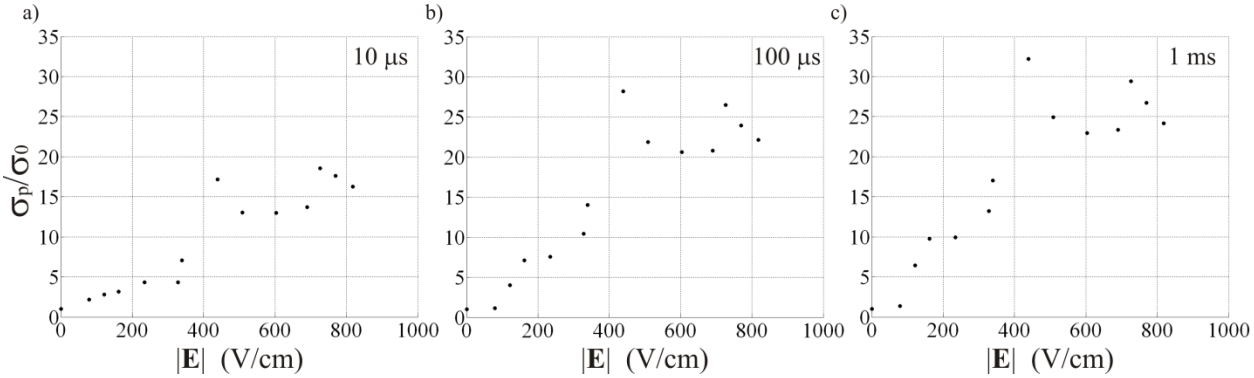

Figure 14. Relative potato conductivity during the application of electric field pulses ranging from 0 V/cm to 820 V/cm . The ratio between the instantaneous conductivity and the conductivity before the pulse is applied is displayed at 10 µs (a), at 100 µs (b) and at 1000 µs (c).

In comparison with animal and human soft tissues the ratio R_0/R_∞ of potato tuber is extremely high. Probably the only exception to this statement is the skin, which has a very low conductivity, particularly when it is dry[21]. Hence it is not too surprising that electroporated skin shows a much higher ratio σ_p/σ_0 at 100 µs than other animal tissues (Figure 15).

In figure 15 it is also interesting to note that muscle seems to reach σ_p/σ_0 saturation for field magnitudes above 600 V/cm whereas at this same field the ratio σ_p/σ_0 in the case of tumors has barely gone above 1. In fact, tumor σ_p/σ_0 only rises above 3 when field magnitude is larger than 2500 V/cm (not published data obtained in collaboration with Prof. L. Mir). These observations indicate how large the difference in electroporation thresholds can be between different tissues. The same can be noticed when the effects of electroporation are analyzed: for the same protocol, 8 rectangular pulses of 100 µs at 10 Hz, irreversible electroporation in muscle is observed at field magnitudes lower than 500 V/cm [56] whereas for sarcoma tumors the threshold seems to be larger than 2000 V/cm [65].

The fact that tissue conductivity depends on the magnitude of the electric field must be taken into account when calculating field distributions: once a high voltage pulse is applied some tissue areas will be electroporated very fast, their conductivities will increase and a redistribution of the electric field magnitude will occur. Since electroporation takes place almost immediately (<10 ns) when the critic transmembrane potential is reached (in about 1µs after the pulse), it can be presumed that the whole process of field redistribution will happen in a few microseconds, that is, in an almost insignificant portion of the pulse (typically 100 µs). This phenomenon has been incorporated in recent FEM simulations of the electric field distribution [66-69]. In these

[21] A comprehensive collection on tissue impedance data can be found in http://niremf.ifac.cnr.it/tissprop/ which is based on the data collected in [62-64].

simulations the electric field magnitude distribution is computed in an iterative process in which in each step the conductivities are adjusted according to the electric field computed in the previous step. Figure 16 shows an example that shows the importance of taking into account the dependence of the conductivity on the field magnitude: when the iterative method is not applied the computed field distribution indicates that the field magnitude within the tumor is very low because of the skin resistance; it would not be capable of electroporation. A lot of experimental and clinical studies on electrochemotherapy [70] indicate that that cannot be the case; electroporation indeed occurs within tumors. Moreover, in a recent paper [71] it was measured the electric field magnitude within tumors and it was found that, although the skin indeed has a significant shielding effect, the actual inner electric field value was in the same order of magnitude than the inner electric field predicted without the influence of the skin.

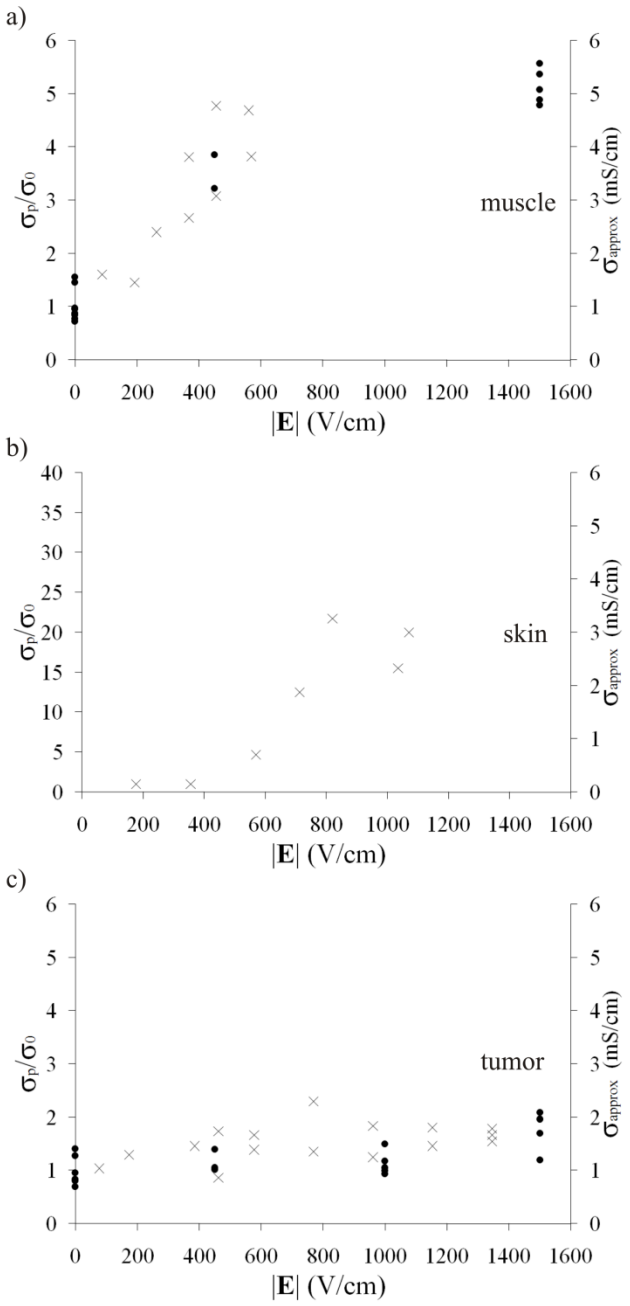

Figure 15. For three different animal tissues (rat transversal skeletal muscle, rat skin and sarcoma tumor implanted in mice), relative conductivity (σ_p/σ_0) at 100 μs after the beginning of the pulse. The approximate absolute conductivity is also represented on the secondary vertical axis (right). The symbol × indicates data from [67] whereas the symbol • indicates data collected by the author (muscle data partially published in [60]).

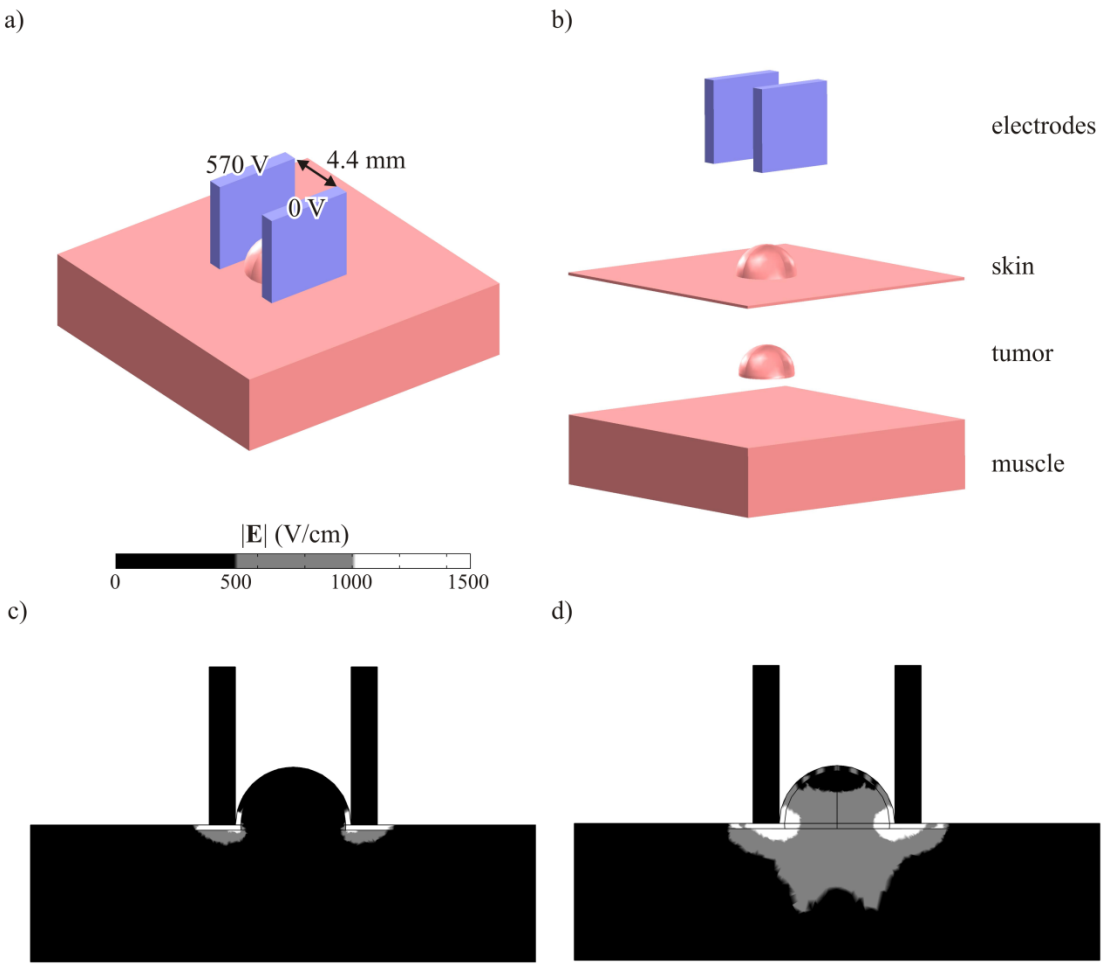

Figure 16. Comparison between the simulation results of the electric field magnitude (|**E**|) distribution when it is assumed that tissue conductivity does not change (c) and when it is assumed that tissue conductivity depends on the electric field and the distribution is computed with an iterative process (d). The first case (c) is completely unrealistic as it would imply that only the skin is electroporated.

6. Conductivity changes induced by electroporation

There are quite a few studies on isolated membranes [26] and on cells [23, 57, 72-77] in which the electrical conductance is measured after the application of the electroporation pulses or in between the application of multiple pulses. From all these studies some interesting general observations can be extracted:

1) After cessation of the high voltage pulse, membrane conductance[22] drops very fast (<<1 ms) to a value which is much smaller than the conductance during the pulse (σ_p) but significantly larger than the conductance value before the pulse (σ_0). This phenomenon is presumably linked to the resealing of short-lived pores and resembles the fast increase in conductance that is observed when the high voltage pulse is applied.

2) After the fast conductance drop, the conductance of the whole sample keeps falling slowly (seconds) towards the original conductance value and, in the case of dense cell suspensions (e.g. cell pellets), it even goes significantly below that original value. This slow recovery of the membrane resistance is associated with the existence of long-lived pores which can last for minutes. Of course, if the pulse is large or long enough, some degree of permeabilization will be irreversible and the original membrane resistance will never be reached. On the other hand, the fact that the resistance can get to values larger than the original one is explained as being the result of osmotic imbalance induced by the permeabilization: water rushes into the cells and causes them to swell so that the extracellular spaces are significantly compressed and, therefore, the resistance at low frequencies increases notably [72].

3) Conductance changes due to multiple electroporation pulses show a memory effect, that is, for each pulse the conductance during and after the pulse depends on the pulses that were applied before. A generally observed phenomenon is that post-pulse membrane conductance increases gradually pulse after pulse.

These phenomena can also be observed in the very few studies in which tissue conductance is assessed after or in between the pulses [55, 60, 78-80]. Due to the large ratio between cell volume and extracellular volume in tissues, the conductance increase caused by electroporation in tissues is much more noticeable than in cell suspensions. As a matter of fact, in some cases the conductance increase observed in cell suspensions is not related to an increase of membrane conductance but to secondary effects such as the release of intracellular contents [57].

Typical conductivity behaviors during tissue electroporation (8 pulses of 100 μs at 10 Hz) can be observed in figure 17. These examples (obtained from [80]) correspond to *in vivo* experiments with rat livers. When the electric field magnitude is 450 V/cm (subfigure a) conductivity slightly increases pulse after pulse up to a value $\sigma/\sigma_0 = 1.08$. The conductivity during the pulses (represented with a single circle) is significantly higher than the conductivity just before or just after each pulse. This *in-pulse* conductivity (σ_p) also shows a quite linear progressive increase. On the other hand, when the magnitude is 1500 V/cm (subfigure b) the in-pulse conductivity

[22] Conductance before and after the pulse is typically measured by means of low frequency (<10 kHz) AC signals of very low amplitude. If the frequency is sufficiently low then the impedance magnitude is very similar to the resistance value at "0 Hz" (see figure 6.b). DC signals are generally avoided because they have an effect on the sample (electrochemical reactions and possible effects on the electroporation process).

seems to saturate at a value (3.2 mS/cm) which is quite close to the pre-treatment admittance value at high frequencies [80]. In this case the conductivity increase induced by each pulse is quite significant and it accumulates up to a conductivity value a 42% higher than the original conductivity ($\sigma/\sigma_0 = 1.42$).

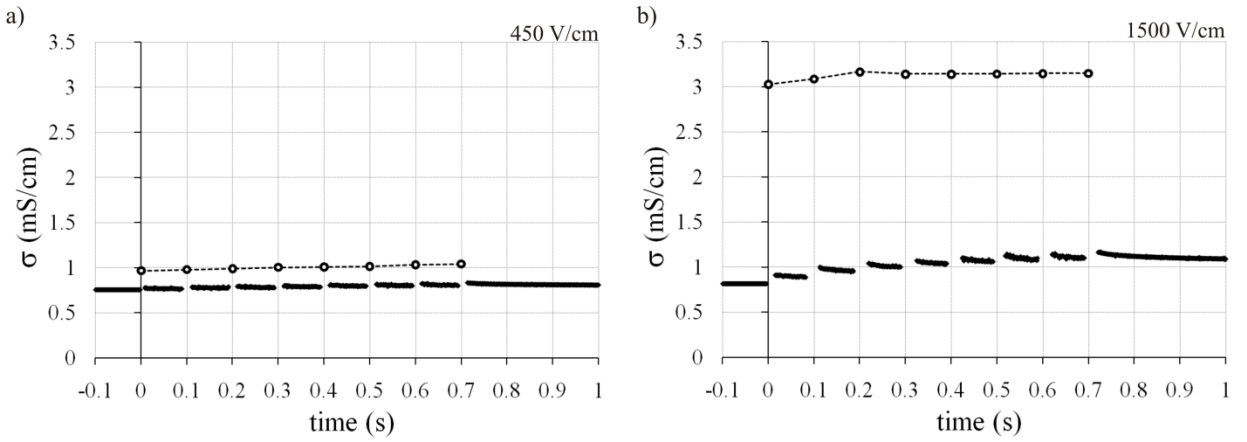

Figure 17. Two examples of conductivity evolution during *in vivo* electroporation of rat liver. Points marked with circles and joined by a dashed line represent the conductivity values obtained at the end of the electroporation pulses (*in-pulse* conductivity, σ_p). The electroporation protocol consisted of 8 rectangular pulses of 100 μs at 10 Hz. In a) the magnitude of the electric field was 450 V/cm and in b) it was 1500 V/cm.

As it would be expected, in all tissue studies reported up to the current date tissue conductivity immediately after the electroporation sequence is larger than the original conductivity. The in-pulse conductivity also seems to increase pulse after pulse, or at least reaches a saturation level and remains stable (Figure 17.b). However, there are two experimental cases in which a decrease of the in-pulse conductivity was observed: irreversible electroporation of rat muscle [60] and rat artery [81, 82]. A plausible, but not demonstrated, explanation to this unexpected phenomenon could be that the voltage pulses cause contraction of the arteries by stimulating the muscle cells (vascular smooth muscle cells in the case of the artery) and that such contraction results in an increase of the electrical impedance [83-85].

The eight 100 μs pulses at 10 Hz with a field magnitude of 450 V/cm is considered to be a reversible electroporation protocol for the rat liver case. On the other hand, when the same protocol is applied with a magnitude of 1500 V/cm the effects are unmistakably irreversible. For instance, in less than two hours after electroporation the area exposed to the electric field shows a very distinctive dark red color that is due to the accumulation of erythrocytes after the destruction of the endothelium of the liver vasculature system. Furthermore, microscopic observations show a very significant increase of the interhepatocyte space that is probably caused by massive cell lysis [80].

Conductance monitoring after the electroporation sequence yields interesting observations (figure 18). The "reversible" protocol (450 V/cm, gray line) induces first a fast, but small (<10%), increase in conductance and then conductance decreases slowly down to a minimum, at about 2 minutes, that is lower than the original conductance value. As indicated earlier, such decrease is thought to be related to the osmotic imbalance induced by the permeabilization [72]. Besides permeabilization, it is possible that another source of osmotic imbalance concurs in this case: tissue electroporation is usually accompanied by reversible blood occlusion [86] which causes ischemia and in turn induces cell swelling [87]. After the minimum, conductance goes up very slowly and reaches values higher than the original value, probably due to some degree of irreversible electroporation (cell lysis) around the electrode edges. Understandably, the "irreversible" protocol (1500 V/cm. black line) shows a much larger immediate increase in conductance (>35%). However, the pattern up to 10 minutes is quite similar to the 450 V/cm case: a minimum after one minute and a tendency to reach quite stable values afterwards. Then, between 10 and 15 minutes, a quite dramatic increase in conductivity is observed that is probably related massive lysis of liver cells.

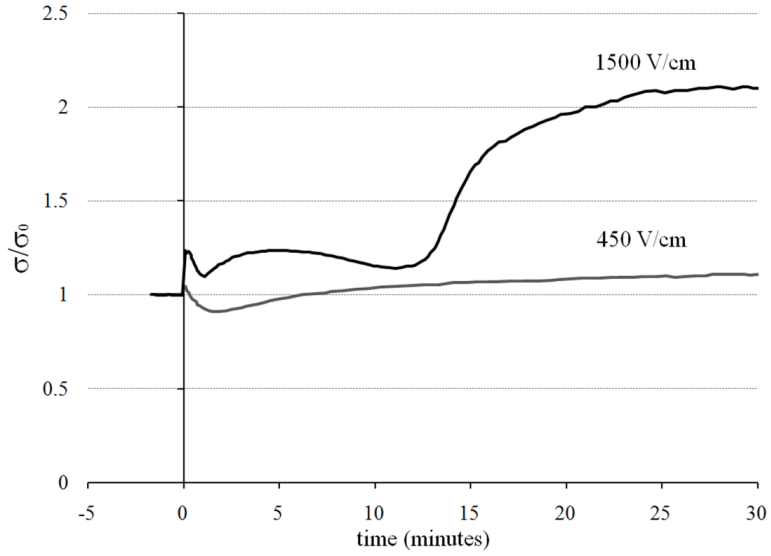

Figure 18. Examples of *in vivo* relative conductivity evolution after electroporation of rat liver. Electroporation (8 rectangular pulses of 100 μs at 10 Hz) is produced at time = 0 minutes. Grey trace is for the case in which the magnitude of the electric field is 450 V/cm whereas the black trace is for a magnitude of 1500 V/cm and it clearly manifests the effect of irreversible electroporation, that is, a remarkable increase in conductivity.

Table 1 summarizes some experimental results in which tissue conductivities are increased by applying an electroporation protocol that consists of 8 pulses of 100 μs at 10 Hz. It is interesting to note the disparity of electric field magnitudes needed to get a certain conductivity increase. For instance, to reach a 40 % increase, 2500 V/cm are needed for tumors whereas for liver only 1500 V/cm are needed and at 450 V/cm in the case of the muscle the conductivity increase is 70

%. Up to a point, irreversible field thresholds and conductivity increases seems to be correlated: in all the examples of the table, 30% or larger conductivity increases coincide with irreversible conditions. However, it must be said that no such a thing as a universal conductivity increase threshold for irreversibility has been found.

$\Delta\sigma$ (50 ms after EP)	EP protocol: 8 pulses of 100 μs separated by 100 ms		
	$\|\mathbf{E}\|$ = 450 V/cm	$\|\mathbf{E}\|$ = 1500 V/cm	$\|\mathbf{E}\|$ = 2500 V/cm
Rat liver	9 ± 3 %	43 ± 5 %	-----
Rat muscle	70 ± 15 %	95 ± 23 %	-----
Mice sarcoma	8 ± 2 %	12 ± 3 %	39 ± 5 %
Potato	78 ± 15 %	-----	-----

Table 1. Experimentally measured increases (mean ± standard deviation) in tissue conductivity after an electroporation sequence that consists of 8 pulses of 100 μs at 10 Hz. Rat liver results are from [80] and rat skeletal muscle results are from [60]. Results from sarcoma tumor implanted in mice and results from potato have been obtained by the author in collaboration with Prof. L. Mir's lab and have not been published yet.

7. Effect of electroporation on other bioelectric phenomena

In all bioelectric phenomena the cell membrane permeability (or better said, its selective permeability) plays a crucial role. Therefore, it seems quite obvious that electroporation can have a significant impact on such phenomena, reversibly or irreversibly. Moreover, the high voltage pulses employed to achieve electroporation can initiate action potentials in muscles and nerves within the region under treatment or in distant areas; it must remembered that the thresholds for excitation are significantly lower than the thresholds for electroporation. As a matter of fact, one of the few drawbacks of electroporation based therapies is that they can cause acute pain and muscle contraction in the vicinity of area where the electrodes are applied. In some cases local anesthesia is enough to minimize discomfort to the patient but in other cases general sedation may be preferred [88] combined or not with muscle relaxants [89].

However, the main immediate concern of clinicians dealing with electroporation is whether the electroporation voltage pulses can elicit ventricular fibrillation (VF) or other cardiac arrhythmias. Such concern is perfectly justified if it is taken into account that cardiac muscle is extremely sensitive to a large variety of electrical stimuli [90]. For instance, it is quite astonishing to learn that currents above 10 A may be used in irreversible electroporation treatments whereas the residual breaker circuit breakers[23] are designed to open its contacts when the leakage current

[23] Residual current circuit breakers, also known as differential breakers or ground fault interrupters, are electrical wiring devices intended to prevent ventricular fibrillation in the case in which a grounded person touches the energized part of a circuit so that a leakage current flows through the body. These devices disconnect the circuit when the electric current is not balanced between the phase conductor and the neutral conductor.

goes above 30 mA. Hence it sounds reasonable that since the beginning of the use of *in vivo* electroporation researchers were worried with the possibility that an electroporation treatment in any part of the body could result in fatal fibrillation due to residual currents flowing through the myocardium. As a matter of fact, a technical solution to this problem was envisioned quite early [91]: voltage pulses can be synchronized with the electrocardiogram signal so that they are delivered when all myocardium cells are in the *absolute refractory period*; in this period it is not possible to initiate action potentials regardless of the amplitude of the excitation signal. This sort of solution has been studied more recently by other researchers [92, 93]. Nevertheless, it appears that the topic has been quite ignored during the 90s and the beginning of the 2000s, when *in vivo* electroporation started to be used clinically for superficial treatments and in animal research for multiple internal treatments. The reason for such oblivion is also understandable: it is not possible to find a single report in which ventricular fibrillation occurred after electroporation, neither in human trials nor in animal experimentation. In the cases in which electroporation was applied to human limbs residual current densities through the heart were probably too weak to induce any effect. On the other hand, when tumors on the chest were treated, and particularly during experimentation with small animals, it is very plausible that current densities above 0.5 mA/cm^2 flowed through the heart[24] and, therefore, VF would have been very likely to occur. However, it must be taken into account that this specific 0.5 mA/cm^2 current density threshold for ventricular fibrillation is applicable for prolonged (> 1s) 50 Hz or 60 Hz exposures but it is meaningless for short pulses as those employed in electroporation. It is a known fact that long exposures at around 50 Hz are the most dangerous ones in terms of VF; lower or higher frequencies imply much larger thresholds and that could explain why VF was never observed in electroporation *in vivo* treatments. Unfortunately, little experimental data exists on stimuli with features similar to those of electroporation pulses and it is not possible to provide here a reliable threshold value. Mali et al. [93] employed a VF threshold from [94] for single DC pulses of 500 μs: total current of 100 mA flowing through the entire heart. This seems a reasonable value as in most of the cases electroporation pulses will be shorter and, in principle, less prone to induce VF. Even so, it is clear that further research is required in this area. For instance, it is necessary to analyze how the fact that multiple pulses are applied can increase the chances of VF and what is the importance of the pulse duration and of the interval between pulses.

In relation to the above paragraph it is interesting to note that Lavee et al. [95] carried out a study with five pigs in which IRE of the atrium was performed for the treatment of atrial fibrillation, as an alternative to methods based on thermal ablation. Pulse sequences with an amplitude of 1500 V or 2000 V, a frequency of 5 Hz and up to 32 pulses were applied and no permanent arrhythmia or any significant rhythm disturbance was observed apart from the rapid pacing imposed momentarily by the sequence of pulses. That study does not contain information regarding electric current measurements but, taking into account the electrode setup geometry (two parallel

[24] Reilly, in (Reilly 1998), compiled results from numerous experimental studies on myocardium stimulation and fibrillation.

4 cm long cylindrical rods of 2 mm in diameter at opposite sides of the tissue with a thickness ranging from 5 mm to 14 mm) and if we assume that the myocardium resistivity during IRE can go down to 300 Ω.cm, we estimate that the current applied in some cases was larger than 20 A. This astonishing result confirms that further research is required in this area.

In relation also with the heart it must be mentioned that quite a few recent research articles are pointing out at the possible role of electroporation on defibrillation therapy [96-104]. In this case the research is not focused on the effect of the electrical stimulus associated with electroporation but on electroporation itself, that is, on the effect of reversible, or irreversible, permeabilization. This topic has been recently reviewed by Nikolski and Efimov in [105] and they conclude that electroporation indeed can affect the outcome of defibrillation and that it can have both pro- and anti-arrhythmic consequences. It is also interesting to note here that it is suspected that electroporation could play a significant role in radiofrequency myocardium ablation [106].

It is generally accepted that electroporation influences action potential generation and transmission by causing a nonspecific increase of cell membrane permeability to ions. The main observable effects of electroporation on excitable cells seem to be: 1) reduction of action potential amplitude and 2) reduction of conduction velocity. For the case of rat sciatic nerve Abramov et al. [107] found that after 75 V/cm shocks (12 pulses of 4 ms at 0.1 Hz) the normal action potential amplitude and conduction velocity were not recovered until 3 hours after treatment, whereas 37 V/cm pulses did not produce significant changes and the changes produced by 150 V/cm were permanent. Comparable transitory muscle incapacitation has been achieved by applying eight 100 μs 300 V/cm pulses [108]. Therefore, it seems very plausible to modulate or to block transitorily, or permanently, conduction in nerves by applying electroporation pulses [109].

References

[1] H. Fricke, "A mathematical treatment of the electric conductivity and capacity of disperse systems. II. The capacity of a suspension of conducting spheroids surrounded by a non-conducting membrane for a current of low frequency," *Physical Review*, vol. 26, 1925.

[2] J. M. Crowley, "Electrical breakdown of bimolecular lipid membranes as an electromechanical instability," *Biophys. J.*, vol. 13, pp. 711-724, 1973.

[3] A. L. Hodgkin, "The ionic basis of electrical activity in nerve and muscle," *Biological reviews of the Cambridge Philosophical Society*, vol. 26, pp. 339-409, 1951.

[4] R. Stämpfli, "Reversible electrical breakdown of the excitable membrane of a Ranvier node," *Anais da Academia Brasileira de Ciencias*, vol. 30, pp. 57-63, 1957.

[5] A. J. H. Sale and W. A. Hamilton, "Effects of high electric fields on microorganisms. 1. Killing of bacteria and yeasts.," *Biochimica et Biophysica Acta*, vol. 148, pp. 781-788, 1967.

[6] W. A. Hamilton and A. J. H. Sale, "Effects of high electric fields on microorganisms. 2. Mechanism of action of the lethal effect.," *Biochimica et Biophysica Acta*, vol. 148, pp. 789-800, 1967.

[7] A. J. H. Sale and W. A. Hamilton, "Effects of high electric fields on microorganisms. 3. Lysis of erythrocytes and protopasts.," *Biochimica et Biophysica Acta*, vol. 163, pp. 37-43, 1968.

[8] K. J. Kinosita and T. Y. Tsong, "Formation and resealing of pores of controlled sizes in human erythrocyte membrane," *Nature*, vol. 268, pp. 438-441, 1977.

[9] E. Neumann, M. Schaeffer-Ridder, Y. Wang, and P. H. Hofschneider, "Gene transfer into mouse lymphoma cells by electroporation in high electric fields," *EMBO J*, vol. 1, pp. 841-845, 1982.

[10] L. M. Mir, S. Orlowski, J. J. Belehradek, and C. Paoletti, "Electrochemotherapy potentiation of antitumour effect of bleomycin by local electric pulses " *European Journal of Cancer*, vol. 27, pp. 68-72, 1991.

[11] L. M. Mir, M. Belehradek, C. Domenge, S. Orlowski, B. Poddevin, J. J. Belehradek, G. Schwaab, B. Luboinski, and C. Paoletti, "Electrochemotherapy, a new antitumor treatment: first clinical trial," *Comptes Rendus de l'Academie des Sciences Serie III Sciences de la Vie*, vol. 313, pp. 613-618, 1991.

[12] S. M. Becker and A. V. Kuznetsov, "Numerical Modeling of In Vivo Plate Electroporation Thermal Dose Assessment," *Journal of Biomechanical Engineering*, vol. 128, pp. 76-84, 2006.

[13] R. V. Davalos, B. Rubinsky, and L. M. Mir, "Theoretical analysis of the thermal effects during in vivo tissue electroporation," *Bioelectrochemistry*, vol. 61, pp. 99-107, 2003.

[14] U. F. Pliquett, G. T. Martin, and J. C. Weaver, "Kinetics of the temperature rise within human stratum corneum during electroporation and pulsed high-voltage iontophoresis," *Bioelectrochemistry*, vol. 57, pp. 65-72, 2002.

[15] J. F. Edd and R. V. Davalos, "Mathematical modeling of irreversible electroporation for treatment planning," *Technology in Cancer Research and Treatment*, vol. 6, pp. 275-286, 2007.

[16] E. Maor, A. Ivorra, and B. Rubinsky, " Intravascular irreversible electroporation: Theoretical and experimental feasibility study," presented at 30th Annual International Conference of the IEEE Engineering in Medicine and Biology Society, 2008. EMBS 2008. , Vancouver, BC, Canada 2008.

[17] G. Pilwat and U. Zimmermann, "Determination of intracellular conductivity from electrical breakdown measurements," *Biochimica et Biophysica Acta*, vol. 820, pp. 305-314, 1985.

[18] A. Ivorra, "Annex A - Bioimpedance monitoring for physicians: an overview. http://www.tdx.cbuc.es/TESIS_UPC/AVAILABLE/TDX-0302105-135356//08Aic08de11.pdf," in *Contributions to the measurement of electrical impedance for living tissue ischemia injury monitoring, PhD Thesis*. Barcelona: Universitat Politècnica de Catalunya, 2005, pp. 131-176.

[19] S. Grimnes and O. G. Martinsen, *Bioimpedance and Bioelectricity Basics*. London, UK: Academic Press, 2000.

[20] F. Riemann, U. Zimmermann, and G. Pilwat, "Release and uptake of haemoglobin and ions in red blood cells induced by dielectric breakdown," *Biochimica et Biophysica Acta*, vol. 394, pp. 449-462, 1975.

[21] J. Teissie and M. P. Rols, "An experimental evaluation of the critical potential difference inducing cell membrane electropermeabilization," *Biophys. J.*, vol. 65, pp. 409-413, 1993.
[22] U. Zimmermann, G. Pilwat, and F. Riemann, "Dielectric Breakdown of Cell Membranes," *Biophys. J.*, vol. 14, pp. 881-899, 1974.
[23] K. J. Kinosita, I. Ashikawa, N. Saita, H. Yoshimura, H. Itoh, K. Nagayama, and A. Ikegami, "Electroporation of cell membrane visualized under a pulsed-laser fluorescence microscope," *Biophys. J.*, vol. 53, pp. 1015-1019, 1988.
[24] I. G. Abidor, V. B. Arakelyan, L. V. Chernomordik, Y. A. Chizmadzhev, V. F. Pastushenko, and M. R. Tarasevich, "246 - Electric breakdown of bilayer lipid membranes I. The main experimental facts and their qualitative discussion," *Bioelectrochemistry and Bioenergetics*, vol. 6, pp. 37-52, 1979.
[25] K. C. Melikov, V. A. Frolov, A. Shcherbakov, A. V. Samsonov, Y. A. Chizmadzhev, and L. V. Chernomordik, "Voltage-Induced Nonconductive Pre-Pores and Metastable Single Pores in Unmodified Planar Lipid Bilayer," *Biophys. J.*, vol. 80, pp. 1829-1836, 2001.
[26] R. W. Glaser, S. L. Leikin, L. V. Chernomordik, V. F. Pastushenko, and A. I. Sokirko, "Reversible electrical breakdown of lipid bilayers: formation and evolution of pores," *Biochimica et Biophysica Acta*, vol. 940, pp. 275-287, 1988.
[27] P. J. Canatella, J. F. Karr, J. A. Petros, and M. R. Prausnitz, "Quantitative Study of Electroporation-Mediated Molecular Uptake and Cell Viability," *Biophys. J.*, vol. 80, pp. 755-764, 2001.
[28] D. Miklavcic and T. Kotnik, "Electroporation for Electrochemotherapy and Gene Therapy," in *Bioelectromagnetic Medicine*, P. J. Rosch and M. S. Markov, Eds. New York: Informa Health Care, 2004, pp. 637–656.
[29] H. Potter, L. Weir, and P. Leder, "Enhancer-dependent expression of human kappa immunoglobulin genes introduced into mouse pre-B lymphocytes by electroporation," *Proc. Natl. Acad. Sci. USA*, vol. 81, pp. 7161-7165, 1984.
[30] S. Sixou and J. Teissié, "Specific electropermeabilization of leucocytes in a blood sample and application to large volumes of cells," *Biochimica et Biophysica Acta (BBA) - Biomembranes*, vol. 1028, pp. 154-160, 1990.
[31] M. Hibino, H. Itoh, and K. J. Kinosita, "Time courses of cell electroporation as revealed by submicrosecond imaging of transmembrane potential," *Biophys. J.*, vol. 64, pp. 1789-1800., 1993.
[32] C. E. Miller and C. S. Henriquez, "Three-dimensional finite element solution for biopotentials: erythrocyte in an applied field," *IEEE Trans. Biomed. Eng.*, vol. 35, pp. 712-718, 1988.
[33] L. Towhidi, T. Kotnik, G. Pucihar, S. M. Firoozabadi, H. Mozdarani, and D. Miklavcic, "Variability of the minimal transmembrane voltage resulting in detectable membrane electroporation," *Electromagnetic biology and medicine*, vol. 27, pp. 372-385, 2008.
[34] M. Pavlin, N. Pavselj, and D. Miklavcic, " Dependence of induced transmembrane potential on cell density, arrangement, and cell position inside a cell system," *IEEE Trans. Biomed. Eng.*, vol. 49, pp. 605-612, 2002.
[35] S. B. Dev, D. Dhar, and W. Krassowska, "Electric field of a six-needle array electrode used in drug and DNA delivery in vivo: analytical versus numerical solution," *IEEE Trans. Biomed. Eng.* , vol. 50, pp. 1296, 2003.

[36] D. Miklavcic, K. Beravs, D. Semrov, M. Cemazar, F. Demsar, and G. Sersa, "The Importance of Electric Field Distribution for Effective in Vivo Electroporation of Tissues," *Biophys. J.*, vol. 74, pp. 2152-2158, 1998.

[37] D. Miklavcic, D. Semrov, H. Mekid, and L. M. Mir, "A validated model of in vivo electric field distribution in tissues for electrochemotherapy and for DNA electrotransfer for gene therapy," *Biochimica et Biophysica Acta*, vol. 1523, pp. 73-83, 2000.

[38] K. Sugibayashi, M. Yoshida, K. Mori, T. Watanabe, and T. Hasegawa, "Electric field analysis on the improved skin concentration of benzoate by electroporation," *International Journal of Pharmaceutics*, vol. 219, pp. 107-112, 2001.

[39] J. Edd, L. Horowitz, R. V. Davalos, L. M. Mir, and B. Rubinsky, "In-Vivo Results of a New Focal Tissue Ablation Technique: Irreversible Electroporation," *IEEE Trans. Biomed. Eng.* , vol. 53, pp. 1409-1415, 2006.

[40] B. Rubinsky, "Irreversible electroporation in medicine," *Technology in Cancer Research and Treatment*, vol. 6, pp. 255-260, 2007.

[41] R. A. Gilbert, M. J. Jaroszeski, and R. Heller, "Novel electrode designs for electrochemotherapy," *Biochimica et Biophysica Acta (BBA) - General Subjects*, vol. 1334, pp. 9, 1997.

[42] A. Ivorra and B. Rubinsky, "Electric field modulation in tissue electroporation with electrolytic and non-electrolytic additives.," *Bioelectrochemistry*, vol. 70, pp. 551-560, 2007.

[43] A. Ivorra, B. Al-sakere, B. Rubinsky, and L. M. Mir, "Use of conductive gels for electric field homogenization increases the antitumor efficacy of electroporation therapies," *Physics in Medicine and Biology*, vol. 53, pp. 6605-6618, 2008.

[44] K. H. Schoenbach, F. E. Peterkin, R. W. I. Alden, and S. J. Beebe, " The effect of pulsed electric fields on biological cells:experiments and applications," *IEEE Trans. Plasma Science*, vol. 25, pp. 284-292, 1997.

[45] K. H. Schoenbach, S. J. Beebe, and E. S. Buescher, "Intracellular effect of ultrashort electrical pulses," *Bioelectromagnetics*, vol. 22, pp. 440-448, 2001.

[46] Y. Sun, P. T. Vernier, M. Behrend, L. Marcu, and M. A. Gundersen, "Electrode microchamber for noninvasive perturbation of mammalian cells with nanosecond pulsed electric fields," *IEEE Trans. NanoBioscience* vol. 4, pp. 277-283, 2005.

[47] D. W. Jordan, M. D. Uhler, R. M. Gilgenbach, and Y. Y. Lau, "Enhancement of cancer chemotherapy in vitro by intense ultrawideband electric field pulses," *Journal of Applied Physics*, vol. 99, pp. 094701, 2006.

[48] W. Frey, J. A. White, R. O. Price, P. F. Blackmore, R. P. Joshi, R. Nuccitelli, S. J. Beebe, K. H. Schoenbach, and J. F. Kolb, "Plasma Membrane Voltage Changes during Nanosecond Pulsed Electric Field Exposure," *Biophys. J.*, vol. 90, pp. 3608-3615, 2006.

[49] P. T. Vernier, Y. Sun, M.-T. Chen, M. A. Gundersen, and G. L. Craviso, "Nanosecond electric pulse-induced calcium entry into chromaffin cells," *Bioelectrochemistry*, vol. 73, pp. 1-4, 2008.

[50] K. H. Schoenbach, R. Nuccitelli, and S. J. Beebe, "Zap," *IEEE Spectrum*, vol. 43, pp. 20-26, 2006.

[51] K. C. Smith, T. R. Gowrishankar, A. T. Esser, D. A. Stewart, and J. C. Weaver, "The Spatially Distributed Dynamic Transmembrane Voltage of Cells and Organelles due to 10-ns Pulses: Meshed Transport Networks," *IEEE Trans. Plasma Science*, vol. 34, pp. 1394-1404, 2006.

[52] A. G. Pakhomov, J. F. Kolb, J. A. White, R. P. Joshi, S. Xiao, and K. H. Schoenbach, "Long-lasting plasma membrane permeabilization in mammalian cells by nanosecond pulsed electric field (nsPEF)," *Bioelectromagnetics*, vol. 28, pp. 655-663, 2007.

[53] R. Benz and U. Zimmermann, "Pulse-length dependence of the electrical breakdown in lipid bilayer membranes," *Biochimica et Biophysica Acta*, vol. 597, pp. 637-642, 1980.

[54] W. Krassowska and P. D. Filev, "Modeling electroporation in a single cell," *Biophysical Jounal*, vol. 92, pp. 404-417, 2007.

[55] U. Pliquett, R. Elez, A. Piiper, and E. Neumann, "Electroporation of subcutaneous mouse tumors by trapezium high voltage pulses," *Bioelectrochemistry*, vol. 62, pp. 83-93, 2004.

[56] D. Cukjati, D. Batiuskaite, F. Andre, D. Miklavcic, and L. M. Mir, "Real time electroporation control for accurate and safe in vivo non-viral gene therapy," *Bioelectrochemistry*, vol. 70, pp. 501-507, 2007.

[57] M. Pavlin, M. Kanduser, M. Rebersek, G. Pucihar, F. X. Hart, R. Magjarevic, and D. Miklavcic, "Effect of Cell Electroporation on the Conductivity of a Cell Suspension," *Biophys. J.* , vol. 88, pp. 4378-4390, 2005.

[58] E. Gersing, "Monitoring temperature-induced changes in tissue during hyperthermia by impedance methods," *Ann NY Acad Sci*, vol. 873, pp. 13-20, 1999.

[59] W. M. S. Russell and R. L. Burch, *The Principles of Humane Experimental Technique*. London: Methuen & Co. Ltd., 1959.

[60] A. Ivorra, L. Miller, and B. Rubinsky, "Electrical impedance measurements during electroporation of rat liver and muscle," in *13th International Conference on Electrical Bioimpedance*, vol. IFMBE Proceedings 17, H. Scharfetter and R. Merva, Eds. Berlin: Springer-Verlag, 2007, pp. 130-133.

[61] I. N. A. Ashie and B. K. Simpson, "Application of high hydrostatic pressure to control enzyme related fresh seafood texture deterioration," *Food Research International*, vol. 29, pp. 569-575, 1996.

[62] C. Gabriel, S. Gabriel, and E. Corthout, "The dielectric properties of biological tissues: I. Literature survey," *Physics in Medicine and Biology*, vol. 41, pp. 2231-2249, 1996.

[63] S. Gabriel, R. W. Lau, and C. Gabriel, "The dielectric properties of biological tissues: II. Measurements in the frequency range 10 Hz to 20 GHz," *Physics in Medicine and Biology*, vol. 41, pp. 2251-2269, 1996.

[64] S. Gabriel, R. W. Lau, and C. Gabriel, "The dielectric properties of biological tissues: III. Parametric models for the dielectric spectrum of tissues," *Physics in Medicine and Biology*, vol. 41, pp. 2271-2293, 1996.

[65] B. Al-Sakere, F. André, C. Bernat, E. Connault, P. Opolon, R. V. Davalos, B. Rubinsky, and L. M. Mir, "Tumor ablation with irreversible electroporation," *PLoS ONE*, vol. 2, pp. e1135, 2007.

[66] D. Sel, D. Cukjati, D. Batiuskaite, T. Slivnik, L. M. Mir, and D. Miklavcic, "Sequential finite element model of tissue electropermeabilization," *IEEE Trans. Biomed. Eng.*, vol. 52, pp. 816-827, 2005.

[67] N. Pavselj, Z. Bregar, D. Cukjati, D. Batiuskaite, L. M. Mir, and D. Miklavcic, "The course of tissue permeabilization studied on a mathematical model of a subcutaneous tumor in small animals," *IEEE Trans. Biomed. Eng.* , vol. 52, pp. 1373, 2005.

[68] D. Sel, A. Macek-Lebar, and D. Miklavcic, "Feasibility of Employing Model-Based Optimization of Pulse Amplitude and Electrode Distance for Effective Tumor Electropermeabilization," *IEEE Trans. Biomed. Eng.*, vol. 54, pp. 773-781, 2007.

[69] A. Ivorra and B. Rubinsky, "Optimum Conductivity of Gels for Electric Field Homogenization in Tissue Electroporation Therapies," in *IV Latin American Congress on Biomedical Engineering, Bioengineering Solutions for Latin America Health*, vol. IFMBE Proceedings 18, C. Müller-Karger, S. Wong, and A. La Cruz, Eds. Berlin: Springer-Verlag, 2007, pp. 619-622.

[70] M. Marty, G. Sersa, J. R. Garbay, J. Gehl, C. G. Collins, M. Snoj, V. Billard, P. F. Geertsen, J. O. Larkin, D. Miklavcic, I. Pavlovic, S. M. Paulin-Kosir, M. Cemazar, N. Morsli, D. M. Soden, Z. Rudolf, C. Robert, G. C. O'Sullivan, and L. M. Mir, "Electrochemotherapy - An easy, highly effective and safe treatment of cutaneous and subcutaneous metastases: Results of ESOPE (European Standard Operating Procedures of Electrochemotherapy) study," *European Journal of Cancer Supplements*, vol. 4, pp. 3-13, 2006.

[71] B. J. Mossop, R. C. Barr, J. W. Henshaw, D. A. Zaharoff, and F. Yuan, "Electric fields in tumors exposed to external voltage sources: implication for electric field-mediated drug and gene delivery," *Annals of Biomedical Engineering*, vol. 34, pp. 1564-1572, 2006.

[72] I. G. Abidor, L. H. Li, and S. W. Hui, "Studies of cell pellets: II. Osmotic properties, electroporation, and related phenomena: membrane interactions," *Biophys. J.*, vol. 67, pp. 427-435, 1994.

[73] K. J. Kinosita and T. Y. Tsong, "Voltage-induced conductance in human erythrocyte membranes.," *Biochimica et Biophysica Acta*, vol. 554, pp. 479-497, 1979.

[74] M. Schmeer, T. Seipp, U. Pliquett, S. Kakorin, and E. Neumann, "Mechanism for the conductivity changes caused by membrane electroporation of CHO cell-pellets," *Phys . Chem. Chem. Phys* . vol. 6, pp. 5564-5574, 2004.

[75] J. Suehiro, T. Hatano, M. Shutou, and M. Hara, "Improvement of electric pulse shape for electropermeabilization-assisted dielectrophoretic impedance measurement for high sensitive bacteria detection," *Sensors and Actuators B: Chemical*, vol. 109, pp. 209-215, 2005.

[76] J. Wegener, C. R. Keese, and I. Giaever, "Recovery of adherent cells after in situ electroporation monitored electrically," *BioTechniques*, vol. 33, pp. 348-357, 2002.

[77] J. Glahder, B. Norrild, M. B. Persson, and B. R. Persson, "Transfection of HeLa-cells with pEGFP plasmid by impedance power-assisted electroporation," *Biotechnology and Bioengineering*, vol. 92, pp. 267-276, 2005.

[78] R. C. Lee, L. P. River, F. S. Pan, L. Ji, and R. L. Wollmann, "Surfactant-induced sealing of electropermeabilized skeletal muscle membranes in vivo," *Proc. Natl. Acad. Sci. USA*, vol. 89, pp. 4524-4528, 1992.

[79] U. Pliquett, R. S. Langer, and J. C. Weaver, "Changes in the passive electrical properties of human stratum corneum due to electroporation," *Biochimica et Biophysica Acta*, vol. 1239, pp. 111-121, 1995.

[80] A. Ivorra and B. Rubinsky, "In vivo electrical impedance measurements during and after electroporation of rat liver," *Bioelectrochemistry*, vol. 70, pp. 287-295, 2007.

[81] E. Maor, A. Ivorra, J. Leor, and B. Rubinsky, "The effect of irreversible electroporation on blood vessels," *Technology in Cancer Research and Treatment*, vol. 6, pp. 307-312, 2007.

[82] E. Maor, A. Ivorra, J. Leor, and B. Rubinsky, "Irreversible electroporation attenuates neointimal formation after angioplasty," *IEEE Trans. Biomed. Eng.*, vol. 55, pp. 2268-2274, 2008.

[83] T. J. Liao and H. Nishikawa, "The variation of action potential and impedance in human skeletal muscle during voluntary contraction," *The Tohoku Journal of Experimental Medicine*, vol. 173, pp. 303-309, 1994.
[84] C. A. Shiffman, R. Aaron, and S. B. Rutkove, "Electrical impedance of muscle during isometric contraction," *Physiol. Meas.*, vol. 24, pp. 213-34, 2003.
[85] V. M. Jackson, S. J. Trout, and T. C. Cunnane, "Regional variation in electrically-evoked contractions of rabbit isolated pulmonary artery," *British Jounal of Pharmacology*, vol. 137, pp. 488-496, 2002.
[86] J. Gehl, T. Skovsgaard, and L. M. Mir, "Vascular reactions to in vivo electroporation: characterization and consequences for drug and gene delivery," *Biochimica et Biophysica Acta*, vol. 1569, pp. 51-58, 2002.
[87] D. Haemmerich, O. R. Ozkan, J. Z. Tsai, S. T. Staelin, S. Tungjitkusolmun, D. M. Mahvi, and J. G. Webster, "Changes in electricel resistivity of swine liver after occlusion and postmortem," *Med. Biol. Eng. Comput.*, vol. 40, pp. 29-33, 2002.
[88] L. M. Mir, J. Gehl, G. Sersa, C. G. Collins, J.-R. Garbay, V. Billard, P. F. Geertsen, Z. Rudolf, G. C. O'Sullivan, and M. Marty, "Standard operating procedures of the electrochemotherapy: Instructions for the use of bleomycin or cisplatin administered either systemically or locally and electric pulses delivered by the CliniporatorTM by means of invasive or non-invasive electrodes," *European Journal of Cancer Supplements*, vol. 4, pp. 14-25, 2006.
[89] G. Onik, B. Rubinsky, and P. Mikus, "Irreversible Electroporation: Implications for Prostate Ablation," *Technology in Cancer Research and Treatment*, vol. 6, pp. 295-300, 2007.
[90] J. P. Reilly, "Cardiac Sensitivity to Electrical Stimulation," in *Applied Bioelectricity: From Electrical Stimulation to Electropathology*, J. P. Reilly, Ed. New York: Springer, 1998, pp. 194-239.
[91] M. Okino, H. Tomie, H. Kanesada, M. Marumoto, K. Esato, and H. Suzuki, "Optimal electric conditions in electrical impulse chemotherapy," *Japanese Journal of Cancer Research*, vol. 83, pp. 1095-1101, 1992.
[92] B. Mali, T. Jarm, F. Jager, and D. Miklavcic, "An algorithm for synchronization of in vivo electroporation with ECG," *Jounal of Medical Engineering & Technology*, vol. 29, pp. 288-296, 2005.
[93] B. Mali, T. Jarm, S. Corovic, M. S. Paulin-Kosir, M. Cemazar, G. Sersa, and D. Miklavcic, "The effect of electroporation pulses on functioning of the heart," *Medical & Biological Engineering & Computing*, vol. 46, pp. 745-757, 2008.
[94] H. Antoni, "Electrical Properties of the Heart," in *Applied Bioelectricity: From Electrical Stimulation to Electropathology*, J. P. Reilly, Ed. New York: Springer, 1998, pp. 148-193.
[95] J. Lavee, G. Onik, P. Mikus, and B. Rubinsky, "A Novel Nonthermal Energy Source for Surgical Epicardial Atrial Ablation: Irreversible Electroporation," *The Heart Surgery Forum*, vol. 10, pp. E162 - E167, 2007.
[96] L. J. Fogelson, L. Tung, and N. V. Thakor, "Electrophysiologic depression in myocardium by defibrillation-levelshocks," presented at Proceedings of the Annual International Conference of the IEEE Engineering in Medicine and Biology Society, 1988.

[97] O. Tovar and L. Tung, "Electroporation of cardiac cell membranes with monophasic or biphasic rectangular pulses," *Pacing and Clinical Electrophysiology*, vol. 14, pp. 1887-1892., 1991.
[98] O. Tovar and L. Tung, "Electroporation and recovery of cardiac cell membrane with rectangular voltage pulses," *The American Journal of Physiology*, vol. 263, pp. H1128-1136, 1992.
[99] S. B. Knisley, W. M. Smith, and R. E. Ideker, "Prolongation and shortening of action potentials by electrical shocks in frog ventricular muscle," *The American Journal of Physiology*, vol. 266, pp. H2348-H2358., 1994.
[100] W. Krassowska, "Effects of electroporation on transmembrane potential induced by defibrillation shocks," *Pacing and Clinical Electrophysiology*, vol. 18, pp. 1644-1660, 1995.
[101] K. A. DeBruin and W. Krassowska, "Electroporation and shock-induced transmembrane potential in a cardiac fiber during defibrillation strength shocks," *Annals of Biomedical Engineering*, vol. 26, pp. 584-596, 1998.
[102] A. Al-Khadra, V. Nikolski, and I. R. Efimov, "The role of electroporation in defibrillation," *Circulation Research*, vol. 87, pp. 797-804, 2000.
[103] T. Ashihara, T. Yao, T. Namba, M. Ito, T. Ikeda, A. Kawase, S. Toda, T. Suzuki, M. Inagaki, M. Sugimachi, M. Kinoshita, and K. Nakazawa, "Electroporation in a model of cardiac defibrillation," *Journal of Cardiovascular Electrophysiology*, vol. 12, pp. 1393-1403, 2001.
[104] E. R. Cheek and V. G. Fast "Nonlinear changes of transmembrane potential during electrical shocks: role of membrane electroporation," *Circulation Research*, vol. 94, pp. 208-214, 2004.
[105] V. P. Nikolski and I. R. Efimov, "Electroporation of the heart," *Europace*, vol. 7, pp. 146-154, 2005.
[106] C. C. Wu, R. W. n. Fasciano, H. Calkins, and L. Tung, "Sequential change in action potential of rabbit epicardium during and following radiofrequency ablation," *Jounal of Cardiovascular Electrophysiology* vol. 10, pp. 1252-1261, 1999.
[107] G. S. Abramov, M. Bier, M. Capelli-Schellpfeffer, and R. C. Lee, "Alteration in sensory nerve function following electrical shock," *Burns*, vol. 22, pp. 602-606, 1996.
[108] T. Clausen and H. Gissel, "Role of Na,K pumps in restoring contractility following loss of cell membrane integrity in rat skeletal muscle," *Acta Physiol Scand*, vol. 183, pp. 263-271, 2006.
[109] R. P. Joshi, A. Mishra, Q. Hu, K. H. Schoenbach, and A. Pakhomov, "Self-consistent analyses for potential conduction block in nerves by an ultrashort high-intensity electric pulse," *Phys Rev E Stat Nonlin Soft Matter Phys*, vol. 75, pp. 061906, 2007.